



# Cartino2D: Scalable and Automated 2D Shallow Water Rainfall-Flood Inundation Modeling up to Very High Resolution for Large Domains

Frédéric Pons<sup>1</sup>, Nabil Hocini<sup>1</sup>, and Pierre-André Garambois<sup>2</sup>

<sup>1</sup>CEREMA, Aix-en-Provence, France

<sup>2</sup>INRAE, Aix Marseille Univ, RECOVER, Aix-en-Provence, France

**Correspondence:** Frédéric Pons (frédéric.pons@cerema.fr)

## Abstract.

While 2D shallow water models with rainfall and infiltration provide a physically consistent framework for flood inundation modeling, their automated application at large scales remains constrained by challenges related to unstructured mesh generation, parameter specifications, and the integration of heterogeneous geospatial and hydrological datasets. This study presents 5 Cartino 2D (C2D), a novel automated framework that enables the large-scale deployment of the well-established Telemac2D model, for solving the complete 2D shallow water equations, with flexible, spatially distributed hydrological forcing—either from rainfall fields or discharge hydrographs. C2D features topography-aware unstructured mesh generation, optional automated handling of hydraulic structures, and spatial parameter estimation from diverse datasets, including land use. It supports multi-resolution simulations up to very high (metric) resolutions and includes optional automated flow analysis at user-defined 10 transects. The framework also features an automatic subdomain sectorization step, based on preliminary simulations on a regular grid, to delineate hydrologically-hydraulically consistent regions and inform targeted unstructured meshing procedures. The framework is successfully applied at the national scale across France, using 100-year return rainfall and discharge values from the SHYREG database, as well as at very high resolution in the complex metropolitan area such as the Aix-Marseille Provence 15 or Grabels City, demonstrating both scalability and robustness. Model outputs are evaluated using flood marks and firefighter intervention records, showing encouraging hydrological and hydraulic consistency. This advancement opens new opportunities for large-scale flood hazard pre-assessment in France and can be transposed to other countries using global and/or national data. Future work will focus on improving culvert representation, testing alternative infiltration models, and extending the framework for model parameter optimization, coastal flooding and real-time applications.

## 1 Introduction

20 Floods are among the most devastating natural hazards, and their frequency and intensity are projected to increase due to climate change and growing population exposure (UNISDR, 2015). Consequently, flood risk has become a critical societal concern in the 21st century. Addressing this challenge requires accurate estimation of flood inundation hazards at specific probability levels, which is fundamental for effective risk reduction strategies. At the same time, high-resolution early warning



systems capable of reliably forecasting flood inundation magnitude and timing are essential for enabling timely and targeted responses. Furthermore, automated modeling frameworks at national and continental scales are necessary to cover large areas that remain unaddressed by local or national flood mapping programs (Ward et al., 2015), a gap that persists even in some highly developed regions such as the United States (Wing et al., 2018).

Thanks to the global availability and increasing resolution and quality of rainfall and terrain elevation (DEM) data—key inputs for flood inundation hydrological-hydraulic modeling e.g. Hocini et al. (2020); Hocini (2022)—flood models have recently expanded to cover regional e.g. Godet et al. (2025), continental, and even global scales (cf. Trigg et al. (2016); Wing et al. (2024) and references therein). Early global flood models (Yamazaki et al., 2011b; Ward et al., 2013; Winsemius et al., 2013) were based on simplified 1D hydraulic models solved at relatively coarse resolution ( $0.25^\circ$ – $0.5^\circ$ ) and applied mass-conservative downscaling for flood mapping at finer resolution, leveraging the global SRTM DEM (Farr et al., 2007). Momentum was also considered for downscaling in CaMa-Flood (Yamazaki et al., 2011a). Studies have highlighted the importance of accurately representing momentum diffusion on floodplains (Yamazaki et al., 2011a) and the detailed geometry of river network channels (Neal et al., 2012).

Second-generation global flood inundation models used zero convective-inertia (cf. (Bates et al., 2010)) 2D hydraulic modeling (Dottori et al., 2016; Sampson et al., 2015) at higher resolutions of around 1km and 90m, respectively. More recently, a 30m resolution global flood model was developed that accounts for coastal boundary conditions, fluvial and pluvial flood hazards at the global scale, and includes effective channel geometry based on backwater curve inversion (Wing et al., 2024), while still employing the zero-convective inertia model following (Sampson et al., 2015). However, neglecting convective inertia limits the applicability of these models to low subcritical flow regimes. Consequently, performing consistent rainfall–flood–inundation modeling using state-of-the-art 2D shallow water solvers—at very high resolution and over large territories often marked by sharp topographic gradients and steep slopes—remains a significant challenge.

Moreover, many existing models rely on regular grids only, which can be limiting in their ability to represent complex terrain features or adapt spatial resolution according to the heterogeneity of the landscape. Regular grids impose a uniform resolution across the entire domain, leading to unnecessary computational costs in homogeneous or low-interest areas and insufficient resolution in regions with intricate topographic variations. In contrast, unstructured meshes offer greater flexibility by allowing locally refined resolution where needed—for instance, to better reflect subtle changes in topography or important hydraulic features—while using coarser resolution elsewhere to reduce computational burden (e.g. Li et al. (2021); Pujol et al. (2024, 2025)). This adaptability makes unstructured meshes particularly well-suited for scalable, high-resolution flood inundation modeling over large and diverse domains. Regarding the integration of hydrology within 2D shallow water hydraulic models, earlier studies have employed weak coupling with external hydrological models (e.g., Nguyen et al. (2016); Pujol et al. (2022)). Recent research has embedded rainfall–infiltration processes directly into 2D shallow water solvers (Ligier, 2016; Li et al., 2021; Kirstetter et al., 2021; García-Alén et al., 2023; Pujol et al., 2025), enabling improved performance in both hydrologic simulation and floodplain inundation mapping at the basin scale. These models typically rely on fine-resolution unstructured meshes to accurately capture complex topography and hydraulic structures.



Furthermore, these studies emphasize the critical role of parameter estimation in such multiscale 2D shallow water hydraulic models accounting for rain and infiltration. For example, initial soil moisture—an important flood-generating factor e.g. (Roux 60 et al., 2011)—is estimated through sequential filtering-based assimilation of satellite-based surface moisture in (García-Alén et al., 2023). Spatially distributed infiltration parameters, also important for runoff production, are estimated using a gradient-based inverse modeling approach at the basin scale in (Pujol et al., 2025), although this adjoint-based approach with DassFlow 2D (Monnier et al., 2016) remains computationally expensive for large domains.

Hence, there is a clear need for automating the application of full 2D shallow water models with hydraulically consistent 65 unstructured meshes over large domains. Doing so while leveraging diverse data sources for parameter estimation remains a significant challenge—one that is addressed in the present study.

Here we present a novel automatic framework, Cartino2D, for rainfall–flood–inundation modeling using a 2D unsteady 70 shallow water model with rainfall and infiltration processes. The framework is scalable across multiple spatial resolutions up to very high resolution, applicable over large domains, and designed to leverage diverse geospatial and hydrological databases.

The core components of the proposed framework include:

- Advanced data processing and iterative geographic, meshing using GMSH (Geuzaine and Remacle, 2009), and modeling procedures, building on previous expert-driven automatic approaches based on simplified models (e.g., ExZeCo (Pons et al., 2010) and Cartino1D (Pons et al., 2014; Hocini et al., 2020)). Optional automatic handling of hydraulic structures, bridges and transects for analyzing simulated discharge can be take into account.
- 75 – A 2D shallow water numerical solver incorporating spatially distributed rainfall and infiltration processes—specifically here, the open-source Telemac-2D software (Hervouet, 2007), which has been adapted for this purpose.
- Finally, a set of diverse and complementary databases that provide critical constraints for both the meshing workflow and the hydrological–hydraulic (H&H) model parameters and boundary conditions.

The proposed C2D framework is explained into detail and demonstrated in multiple resolutions and configurations, over a 80 urban area at very high resolution and at country scale over France. It builds upon several well-established and powerful open-source libraries, including R (R Core Team, 2021), RStudio (Posit team, 2025), GRASS GIS (GRASS Development Team, 2022), QGIS (QGIS Development Team, 2025), and GDAL (contributors, 2025).

Initial insights into the C2D-Rain methodology are presented in Pons et al. (2021), focusing on the generation of meshes at a local scale using GMSH. Subsequent studies by Pons et al. (2022) and Pons and Hocini (2023) have refined parameter 85 specifications and advanced the integration of heterogeneous geospatial and hydrological databases, as well as the utilization of regular meshes. The application of 2D models in Pons et al. (2024) marked the first operational implementation of the C2D Discharge methodology.

This article is structured as follows. Section 1 introduces the context and motivation for the study. Section 2 provides an 90 overview of the C2D framework, offering a concise glimpse into its core features. Section 3 details the methodology, including the input data and the key processing steps involved in the C2D workflow. Section 4 presents illustrative case studies, including



a nationwide flood inundation model over France, as well as very high-resolution applications over Marseille Métropole and the city of Grabels, principal subdomain used in the description of the method.

## 2 Cartino 2D at a glimpse

The C2D framework is designed to offer automatic and high-resolution 2D unsteady shallow-water (SW) hydraulic modeling for runoff and flooding over extensive areas with structured or unstructured meshes. It leverages multi-source data and a 2D hydraulic numerical model accounting for rain and infiltration to achieve this, with the potential domain size, spatial resolution, and accuracy of the modeling being influenced by both the availability of data and computational resources. The framework supports two primary modeling strategies required for large domains:

- **Cartino "Rain" (C2D-Rain):** Focuses on local runoff modeling.
- 100 – **Cartino "Discharge" (C2D-Discharge):** Focuses on flooding in downstream rivers.

C2D is a versatile tool for both broad and detailed hydraulic modeling applicable at multiple scales, as illustrated in figure, from national level to street scale:

- **Country Scale:** C2D can be applied to model runoff and flooding across an entire country, providing a broad overview of potential flood risks and water dynamics (Section 4.1).
- 105 – **Basin-Floodplain Scale:** The framework can also be used to focus on specific basins or floodplains, offering detailed insights into localized flooding patterns and impacts (Section 4.2).

The primary input data for C2D is high-resolution topography, which is crucial for accurate modeling. Other parameters of the unsteady 2D SW model, such as friction and boundary conditions (including rain and discharge inflows), can be set as constants or spatialized using available data. Both types of C2D modeling strategies—C2D-Rain and C2D-Discharge—rely 110 on the same core data inputs. Additionally, the model can incorporate supplementary data, such as the automatic handling of hydraulic structures, control sections, and land use, with the option to spatialize hydraulic friction and infiltration coefficients. A comprehensive diagram, illustrated in Fig. 2, outlines all the data types that C2D can manage, along with the various processes and subprocesses involved. These processes are further detailed in the subsequent sections.

Cartino2D is protected at the APP. The APP is a European organization for the protection of authors and publishers of digital 115 creations, since 1982. Cartino2D open source code is available on Github repository.

## 3 Methodology: input data and processing steps

The C2D framework presented here is seamlessly integrated with Telemac2D (Hervouet, 2007; EDF R&D, 2014) (T2D), a widely used and robust numerical model for simulating free-surface flows in hydraulic research and engineering applications, enabling effective parallel simulations here with the finite element solver of the 2D shallow water equations. Its versatility

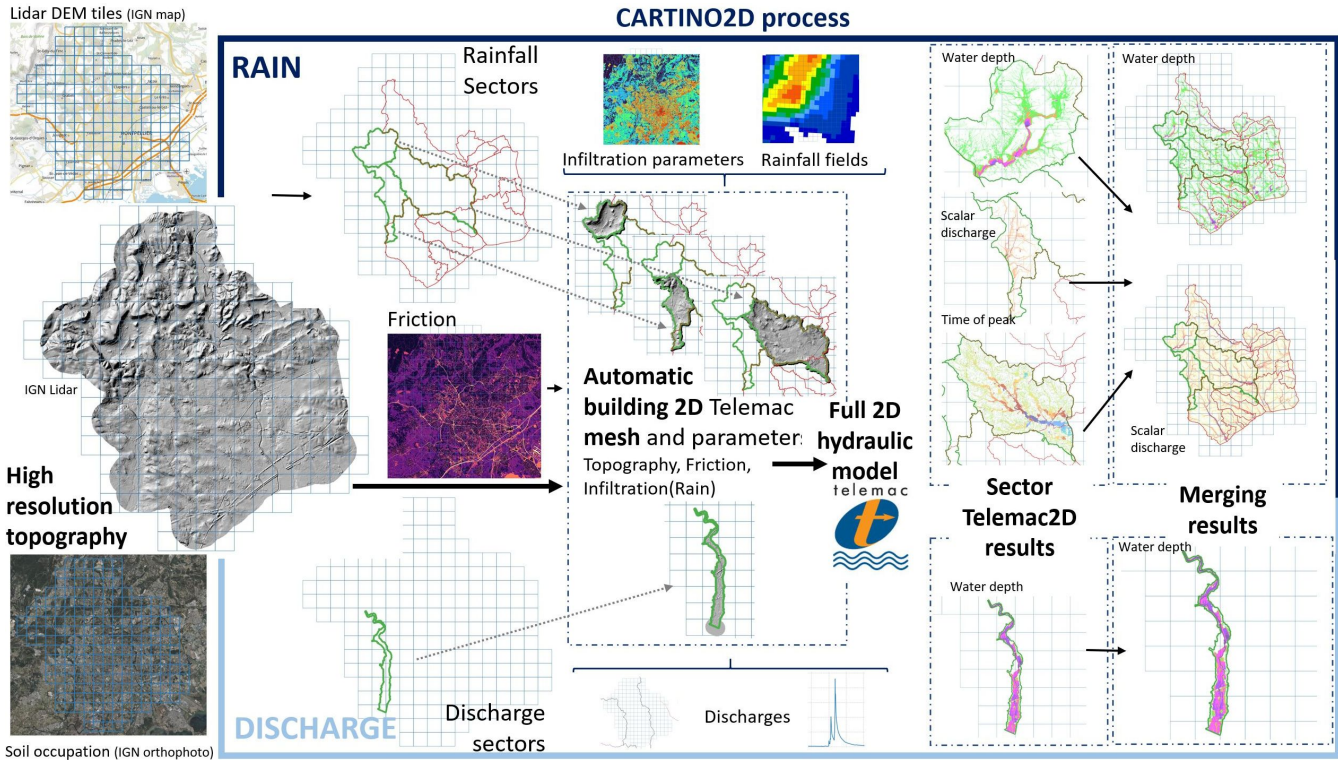


**Figure 1.** Flowchart of Cartino2D process: from input data to flood maps with C2D-Rain process for rainfall-runoff-inundation modeling on upstream catchments and C2D-Discharge for flood-inundation modeling over larger rivers and floodplains.

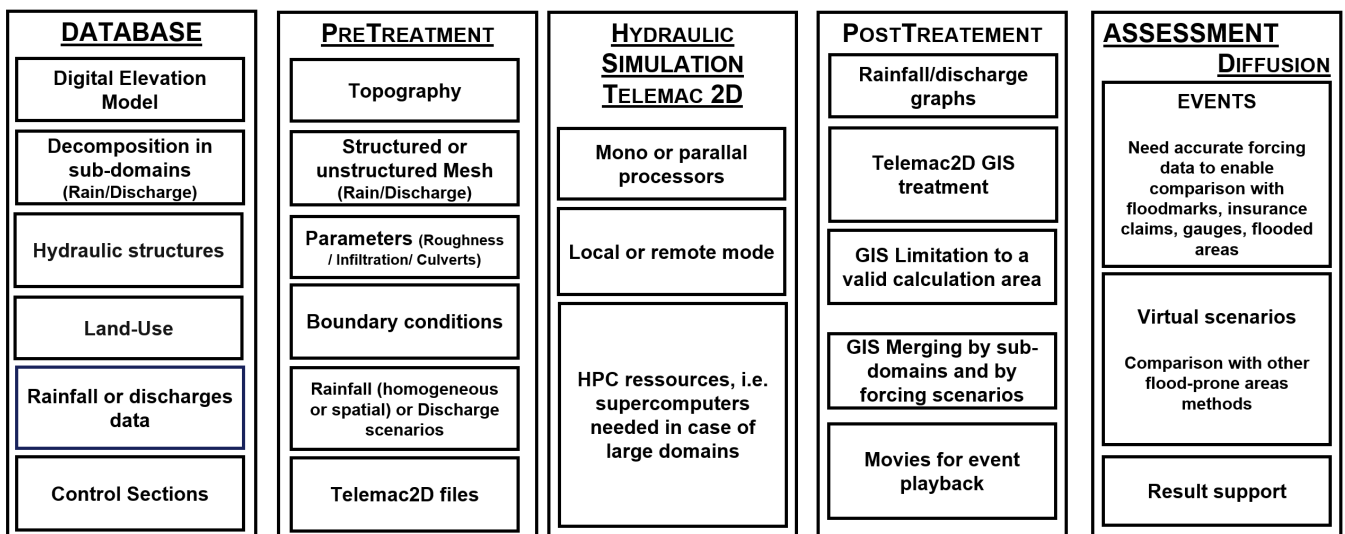


**Figure 2.** General functional diagram of C2D with main input data, sub-processes, outputs and main uses.



120 enables a broad range of simulations, including hydrodynamics of flood inundations, while effectively capturing complex interactions with topography. C2D utilizes GMSH (Geuzaine and Remacle, 2009) and PPUTILS (Prodanovic, 2017) for automatic unstructured mesh generation, providing efficient and flexible discretization of the computational domain, essential for accurate and scalable simulations in both structured and unstructured mesh environments or an home-made square mesh grid.

125 Below, we outline the set of C2D parameters that can be managed automatically to generate a T2D model for each subdomain, maximizing the capabilities of T2D.

To achieve this, C2D integrates a diverse set of databases, leveraging multisource input data categorized into two levels: minimal requirements for basic functionality and optional/maximal requirements for enhanced accuracy and detail.

#### – Common Requirements

- **Digital Terrain Model** (DTM) with its C2D processing (Section 3.1).
- **Hydraulic friction coefficient**: Either a unique value or an optional spatialized raster map (Section 3.4).
- **Key simulation parameters**:

- **Simulation duration**, based on the forcing duration and subdomain size.
- **Time step**, determined by the mesh resolution and simulated flows.
- **Listing printout period**, used for log file analysis and stability assessment.
- **Graphic printout period**: Typically, only the final simulation state is stored to analyze the *maximum* values (C2D-Rain) or the *stabilized* state (C2D-Discharge for steady flows) of the flood area, reducing file size. More frequent exports may be used for temporal analysis.
- **Output variables** at each graphic printout, including standard variables such as water depth, velocity, water level, Froude, peak time (C2D-Rain), and scalar flow rates.

#### 140 – C2D-Rain Minimal Requirements

- **GIS-based subdomain decomposition into multipolygons**. The subdomains are defined by hydrological-hydraulic catchments that constitute the drained area of the study zone. These study subdomains correspond to rainfall subdomains, as illustrated in Fig.1. Further details on the automatic delineation of these subdomains are provided in Section 3.7.
- **SCS curve number model inputs**: uniform or spatially distributed rainfall data, antecedent moisture conditions (Section 3.2), and a uniform or spatially distributed CN (Section 3.4).

#### – C2D-Discharge Minimal Requirements

- **GIS-based subdomain decomposition into multipolygons**. The subdomains are defined by major riverbeds. Further details on the automatic delineation of these subdomains are provided in Section 3.7.
- Discharge inflows with either constant or time-varying hydrographs (Section 3.3).



### – Other Optional Inputs

- Hydraulic structures (Section 3.5).
- Control sections (Section 3.6).

## 3.1 Topography and meshing procedure

155 In this Section, we focus on explaining the automatic generation of 2D hydraulic meshes and their associated parameters. C2D preprocessing starts by domain decomposition for rainfall or discharge and will be described in details, for only one subdomain in each case, in Section 3.7. Recall that the quality of results depends, among other factors, on the quality of the topography data (Hocini et al., 2020) and an open source tool called FILINO has been developed to handle very high resolution Lidar DEM that may require filtering, for example over water bodies.

160 To fully automate the hydraulic simulations, it is essential to manage boundary conditions effectively. The management of topography and meshes is interconnected and is explained for both C2D-Rain and C2D-Discharge scenarios. The objective is to handle the topography around the area of interest to apply the "prescribed elevations for the liquid boundaries T2D option. Topography near the boundaries is modified using different approaches for C2D-Rain and C2D-Discharge.

165 For both C2D-Rain and C2D-Discharge, topography is applied to the meshes as the average of DTM (LiDAR) elevations within each cell for regular meshes, and as the nearest elevation point from mesh nodes (as required by the finite element solver used to resolve the 2D shallow water model) for GMSH-generated, irregularly refined meshes.

### 3.1.1 Cartino2D Rain

C2D-Rain is designed for efficient and consistent runoff modeling over large domains. The meshing strategy employs domain decomposition into complementary subdomains, addressing key challenges such as: (i) preventing unphysical placement of 170 domain boundaries relative to topographic crest lines and catchment limits, including proper handling of flat areas on ridgelines, and (ii) ensuring optimal complementarity between computational subdomains while avoiding issues of overlap, which are kept to a minimum.

175 For each subdomain in C2D-Rain, which corresponds to an a priori defined (but initially unknown high-resolution flowpath) sub-basin or subcatchment, where a sub-basin refers to a larger subdivision of a basin, and a subcatchment is a smaller, hydrologically defined area that drains to a specific point or stream, the meshing strategy is as follows (schematized in Fig.3):

1. **Buffer contour creation:** A larger buffer ( $+d1 = 150m$ ) is applied around the cyan polygon to smooth the boundary and facilitate the meshing of the T2D model (magenta line). This buffer ensures that the boundary does not cut across critical topographic features.
2. **Buffer for postprocessing:** A smaller buffer is then applied from the boundary with  $-d2 = -100m$ , ensuring that  $d2 < d1$ . This buffer, represented by the green line, is used for postprocessing and ensures smooth transitions between the areas of interest (see Fig.3).

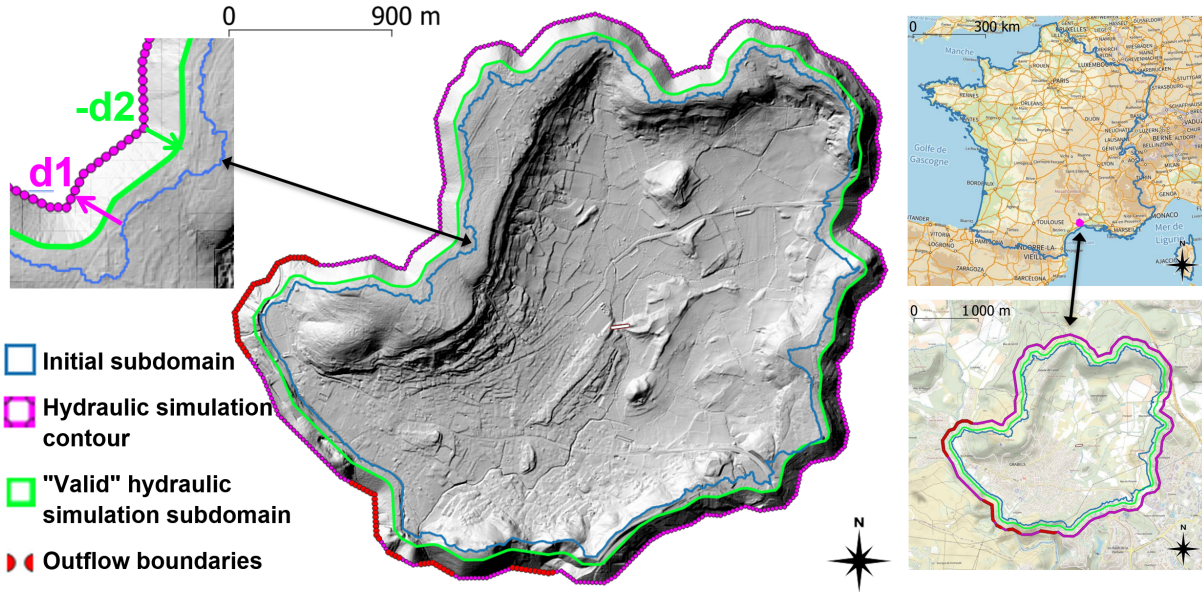


**Figure 3.** Domain contour management for C2D-Rain. The initial subdomain is shown by the cyan line. The hydraulic simulation contour is defined by the  $+d1$  buffer (magenta line), with automatic boundary outlets marked in red. The "valid" hydraulic simulation subdomain for postprocessing is indicated by the  $-d2$  buffer (green line). The topography is shown as a grey hillshade, with local artificial modifications applied to the topography between the hydraulic contour (magenta line) and the "valid" limit (green line) to properly manage boundary conditions. (Right) IGN maps @IGN showing the location of Grabels, a city near Montpellier, France.

185

3. **Topographic Modification (outside green validity domain):** Between the green and magenta lines, the topography is adjusted with an outward slope. The topography within this zone varies from 0 at the green line to  $dZ = -25m$  (default value) at the magenta line. This outward slope is designed to gradually modify the topography, allowing for a smooth transition between the boundary conditions.

4. **Prescribed water surface elevation for downstream boundary condition  $Z_{bc}$ , is calculated as:**

$$Z_{bc} = \max(Z_{min} + dZ_{add}, MSL) \quad (1)$$

190

where  $Z_{min}$  m is the lowest topography value within the postprocessing contour (green one - Fig.3), with  $dZ_{add} = 0.1m$  (default value) added to stabilize the waterline at the downstream boundary.  $MSL = 0.5m$  (default value) is the minimum elevation relative to sea level (for sea-related domains).

5. **Automated definition of boundary conditions (BCs):** The modification of the topography between outer and outside postprocessing buffer is essential for managing the automated definition of boundary conditions, particularly for defining liquid boundaries (represented by the red lines) where prescribed elevations will be imposed as explained after. This ensures that the hydraulic model can appropriately simulate the flow dynamics at the boundaries, with smooth transitions



195 into the domain. The automatic outlet is defined by analyzing altitude points along the domain's contour. Any points with an altitude lower than  $Z_{bc}$  are used to define the outlet.

6. **Initial condition** the water level  $Z_{bc}$  of the boundary condition is imposed on the entire calculation domain. With the definition in Eq. 1, this creates wet cells around the downstream zone mostly outside the validated contour and dry initial condition elsewhere.

200 By following this strategy, the C2D-Rain framework can efficiently handle complex topography and boundary conditions, leading to accurate runoff modeling within a subdomain.

Two types of meshes are used for a single polygon that defines the hydraulic domain, ensuring no holes or unmeshed islands (Fig.4):

205 – **Large Domain Mesh:** A grid mesh, typically composed of two triangles per square, is primarily used for larger domains and during pre-processing (sectorization into subdomains). This mesh is created using a home-made mesher that generates a squared grid from raster data, with triangles obtained by diagonalizing the squares. A step size of 25m is commonly used, but this can also match the native LiDAR DEM resolution (e.g., 1m). Isolated pixels (just 1 or 2 consecutive pixels on a horizontal or vertical line) are deleted to produce a smooth mesh.

210 – **Refined Mesh (C2D-Rain):** This is an unstructured mesh generated by GMSH, with constraints applied along predefined flood-prone areas. The boundary is discretized with a constant step size of  $ds_0 = 25m$  (magenta line). Flood-prone areas are predefined (either by the user, external run, or a large domain C2D simulation see details in appendix A), with close polygons discretized at  $ds_1 = 3m$ . Buffers are applied as follows:

215 –  $dbuf_2 = 10m$ , discretized at  $ds_2 = 10m$   
–  $dbuf_3 = 20m$ , discretized at  $ds_3 = 20m$ . Priority is given to non-intersection between brown polygons ( $ds_1 > ds_2 > ds_3$ ). Orange points are retained, while red ones are excluded (Fig.5). Large cells are used over hills to ensure accurate runoff modeling and reduce noise in simulated fields. Meanwhile, refined mesh areas are concentrated along the talweg to ensure precise hydrological-hydraulic computations.

Finally, this strategy ensures consistency in hydraulic simulations across subdomains, allowing raster results to be seamlessly aggregated (maximum in overlap zones) to generate comprehensive runoff maps for large domain.

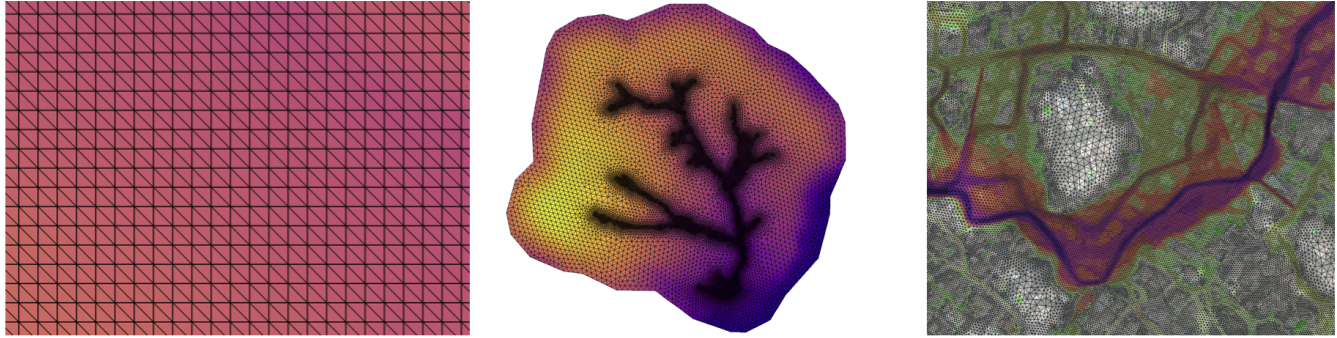


**Figure 4.** Types of meshes usable in C2D Rain: Square Mesh Grid (left), and unstructured mesh over a small catchment (middle) zoomed-in view of an unstructured mesh over a more complex topography in an urbanized area (right).

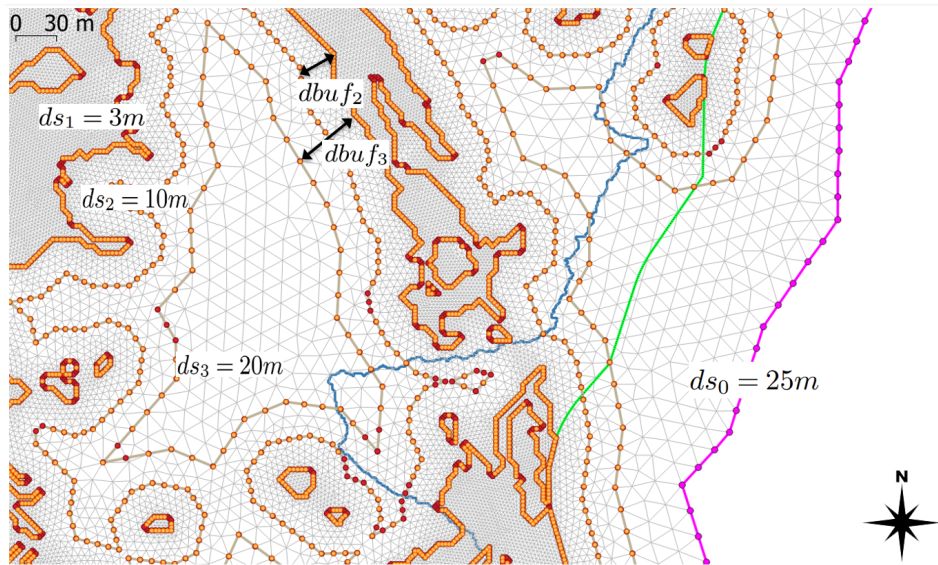


**Figure 5.** Automatic unstructured meshing densified along talwags, using GMSH construction points placed along constraint lines. Initial subdomain (cyan), Hydraulic contour with points each  $ds_0$  m (magenta) and "valid" limit (green). Interior points, predefined from flood prone area contour with successively larger discretization ( $ds_1 = 3m$ ,  $ds_2 = 10m$ ,  $ds_3 = 20m$ ), injected into GMSH and imposing mesh refinement (orange). Those buffer lines are defined from first contour at a distance of  $dbuf_2$ ,  $dbuf_3$  around the predefined flood prone area. Red points are ignored (bad cuts). finite element meshes (gray). Zoom on Grabels area, cf. Fig.3.



## 220 3.1.2 Cartino2D Discharge

C2D-Discharge is designed for efficient flood modeling over large downstream domains over talwags and larger rivers and floodplains, using a dedicated strategy. The process involves the following steps:

1. **Hydraulic simulation contour:** A first buffer with a value of  $+d1 - d2$  meters is applied to the initial subdomain. This buffer defines the boundary for the postprocessing "valid" hydraulic simulation subdomain, represented by the green line. The lower points of the contour are set to be below a minimum elevation  $Z_{bc}$  using Eq. 1 as in C2D-Rain. A contour is then created around these lower points, with a  $+d1$  meter buffer (orange grid area). The two polygons (green and orange) are merged to form the hydraulic simulation contour. The merged contour is discretized at intervals of  $ds_0$  meters (as shown in Fig.6).
2. **Topography Modification:** The topography is modified only around the lower part of the boundary, outside the valid simulation area. In this region, the terrain is flattened, and the elevation is set to the minimum topography value on the contour lowered of  $dZ = -25\text{m}$ .
3. **Elevation prescriptions for BC and IC:** follows the same approach as in *C2D-Rain* and Eq. 1 is used for downstream BC.

Two types of meshes are also available:

- **Large Domain Mesh:** as for C2D Rain, A grid mesh is used, where each square is divided into two triangles, is primarily used for large domains.
- **Refined Mesh :** The mesh refinement procedure is based on the pre-calculation of local DEM curvature using the GRASS tool's *r.param.scale* method ("longc") in 2D, with a neighbor length of  $dx = 5$  meters. A user defined threshold on local topography curvature is applied to identify polygons with rugged topography (non-planar) versus flat topography. The refinement strategy follows the same approach as C2D-Rain, with segmentation applied at intervals of  $ds_1 = 3$  meters,  $ds_2 = 10$  meters, and  $ds_3 = 20$  meters. These segments are applied to the contour polygons with buffers  $dbuf_2$  and  $dbuf_3$  on the rugged topography polygons.

## 3.2 Rainfall data

C2D has been specifically designed to incorporate spatialized rainfall, which is crucial for accurately simulating runoff generation and flood patterns. This enhancement was made possible by modifying the T2D software, which previously supported only punctual hyetographs from rain gauges or uniform rainfall. The modification now enables the ingestion of spatialized rainfall fields, significantly improving the model's ability to simulate complex, geographically varying rainfall events (Hocini and Pons, 2024). This module is freely available on the development branch named MUFFINS in the OpenTelemac GitLab repository.

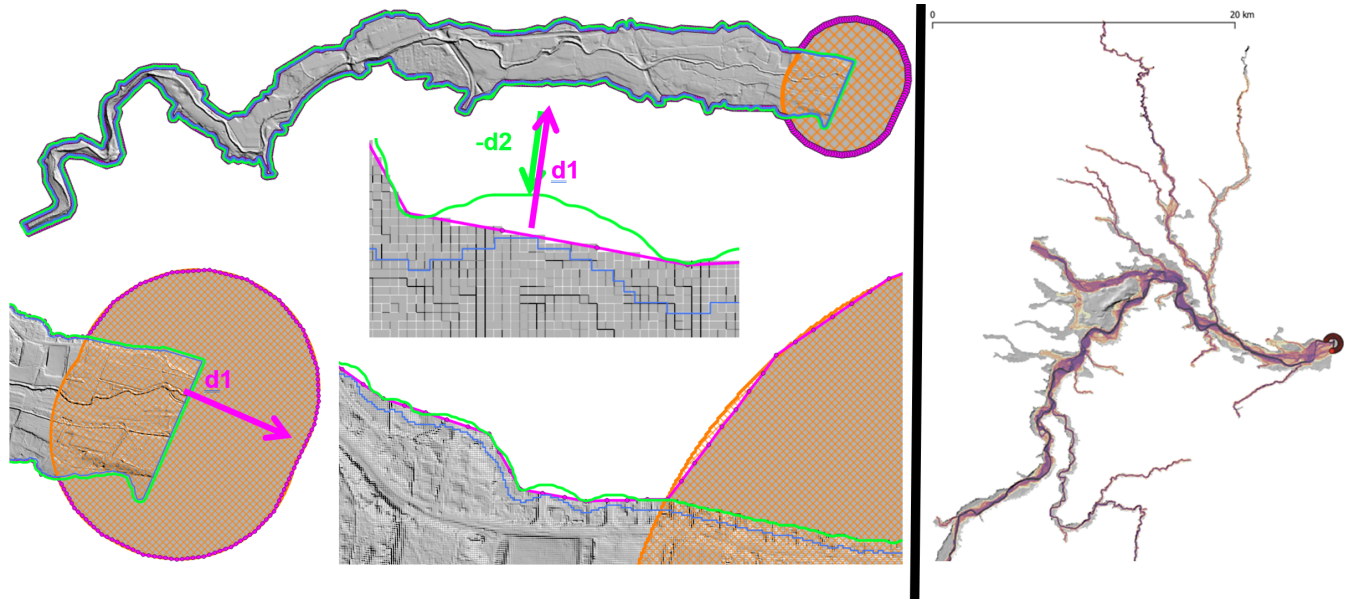


**Figure 6.** Domain contour management for Cartino2D Discharge. Easy case (left) - Initial subdomain (cyan line), limit for postprocessing "valid" hydraulic simulations subdomain with  $+d1 - d2$  buffer (green line), Hydraulic contour for simulation with  $+d1 - d2$  m buffer (magenta line) +  $+d1$  m on the low point of "valid" hydraulic and segmentize each  $ds_0$  m, topography (grey hillshade) with local artificially modified topography to manage boundaries conditions between hydraulic contour and "valid" limit (magenta and green); "Complex" case (right)

250 C2D-Rain is compatible with a variety of rainfall inputs, including radar-derived fields, rain gauge measurements, atmospheric model outputs, or even synthetic rainfall generated from statistical methods for flood inundation hazard characterization.

In this study, C2D-Rain is applied to two types of analyses across France, using both radar-based rainfall data and statistical rainfall products.

255 

- **Events reanalysis** using ANTILOPE J+1 Météo-France product (Champeaux et al., 2009), a radar-gauge reanalysis at 1km spatial and 1h temporal resolutions, disaggregated to 15min temporal resolution. For the most recent years, this product is directly available at a 15min resolution.

**– Runoff-Flood predetermined** using SHYREG database of rainfall and discharge quantiles for the studied region, with a spatial resolution of 1 km for each duration and each return period from (Aubert et al., 2014).

260 The spatialized rainfall database SHYREG can be used for defining a centered or off-centered single-frequency hyetograph (Fig.7). It is, of course, possible to input simple and homogeneous hyetographs over the entire area from record rainfall data or local analyses. We have observed that the shortest rainfall duration is crucial for reproducing rainfall events, especially in upstream watersheds. We work with a minimum time step of 15 minutes. Accurate reproduction of flood events, particularly

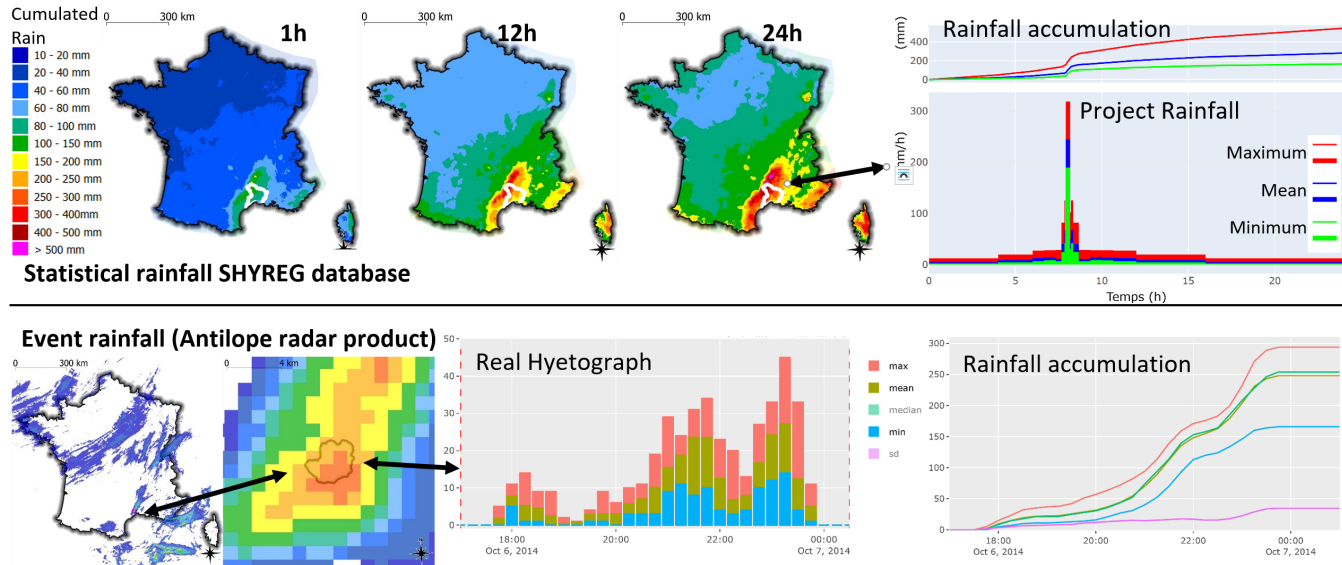


**Figure 7.** Spatialized rainfall products usable in cartino 2D, here for C2D-Rain subdomains. (Top left) Maps of statistical rainfall from SHYREG database (INRAE, Aubert et al. (2014)) and (top right) project hyetograph over Gardon-Nîmes-Montpellier area investigated in Fig.12. (Bottom) Antilope J+1 radar-raingauge rainfall product (Meteo France, Champeaux et al. (2009)) over Grabels area (cf. Fig.5) and time series of spatial statistics.

in upstream watersheds, has been observed to be highly dependent on the temporal resolution of rainfall data, specifically for  
 265 short durations. Consequently, a minimum time step of 15 minutes is employed in the simulations.

### 3.3 Discharge data for C2D-Discharge inflows

To enable the handling of multiple inflow hydrographs, discharges are directly imposed at internal points within the mesh rather than at domain boundaries. Numerical checks (control Section in T2D) confirm that hydraulic modeling consistency is preserved, even when significant discharge is injected into a single hydraulic cell.

270 GIS inflow points file can be created manually or can be extracted from the SHYREG discharge database.

The manual case requires creating inflow points and associated discharge text files. We can use steady or unsteady discharge with statistical or in situ value. Steady or unsteady discharges with statistical or in situ values can be used.

The SHYREG statistical peak discharge database enables to launch the simulation of C2D-Discharge in "steady" mode. SHYREG peak discharge database provides a value of discharge at each pixel of 50m of the river network everywhere in  
 275 France for different return periods. Peak flow increases downstream. Downstream of the confluences, the statistical flow for a return period is logically lower than the sum of the two upstream flows for the same return period. A tool has been developed to extract the inflow points from the SHYREG discharge database. In this context, an inflow point is defined as a location where the statistical discharge—based on SHYREG data—shows a significant increase downstream, indicating the confluence of an

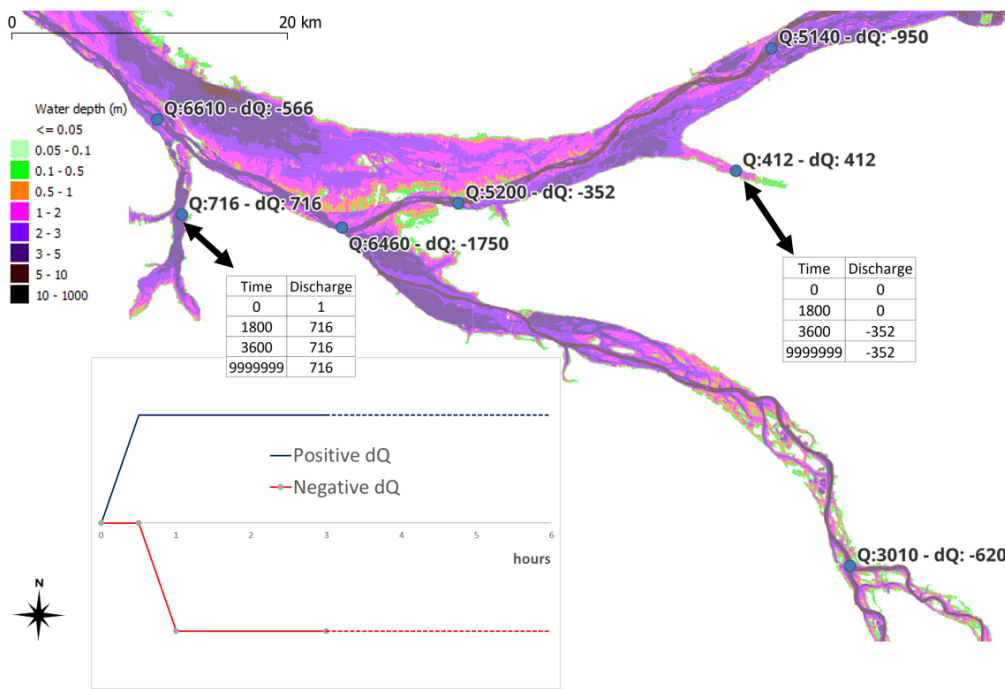


**Figure 8.** Boundary conditions in the 2D hydraulic model are based on SHYREG-derived peak discharges corresponding to a 100-year return period (Q100). Model inputs consist of peak flow differences (dQ), representing positive tributary inflows or negative adjustments at confluences to ensure consistent flow frequency throughout the river network.

upstream basin or sub-catchment. The threshold for this increase is defined as a relative rise in discharge, typically ranging 280 from 5% to 20%, depending on the basin size (with smaller thresholds for larger basins, and vice versa). This methodology has been applied in the development of the national flood inundation mapping framework in France (cf. Fig. 8).

We only retain the results at the end of the simulation, so that we don't have to worry about physical inconsistencies during the simulation. The impact/instability due to strong injection is very localized in a small areas around the injection points. The injection method for peak flow should be applied cautiously in regions with significant flood attenuation. While the 285 presented toolchain allows for dynamic coupling between C2D-rainfall and C2D-discharge, its application in complex flow zones warrants further investigation.

### 3.4 Spatialization of Strickler Friction and Curve Number Runoff Generation Parameters (optionnal)

As said before, the hydraulic roughness and runoff generation parameters can be used as a unique value on the whole domain. Nevertheless, it is better to try to spatialize the data. More and more A multitude of land-cover databases are now available 290 freely and updated. Many of these databases can be used to determine some physical parameters of 2D shallow water models as the roughness (Strickler) or runoff parameters (e.g. Curve Number of SCS method here).

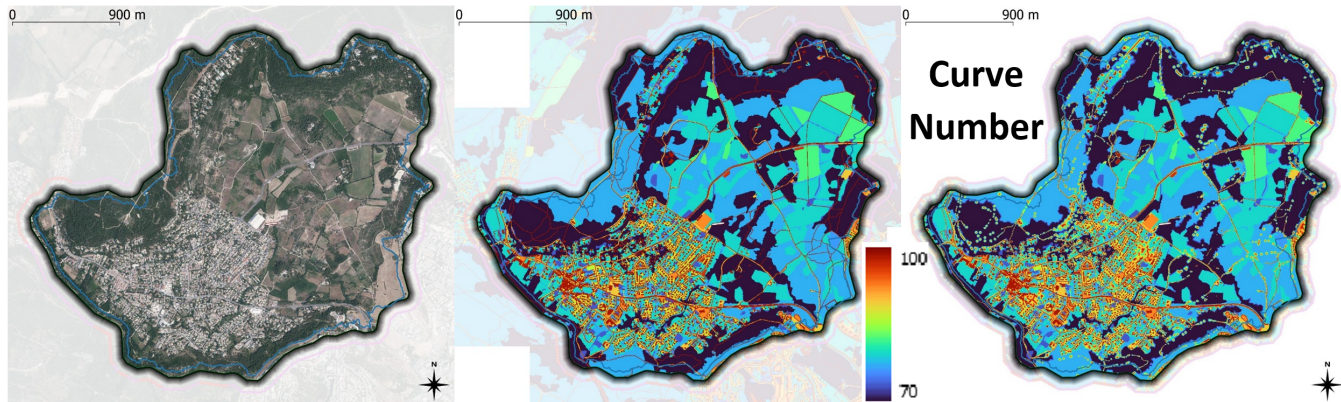


**Figure 9.** Example of Curve Number of Grabels city - left: Ortho IGN, ©IGN. - middle: CN spatialisation database at 1m resolution - right: CN in the C2D mesh, some small patterns (road for example) out of the main flowpath are lost due to resampling (Fig.3)

For these two parameters, the process is to use different land-cover databases, from the most accurate (but not always complete) to the least accurate databases. A manual option is provided to add our own polygon GIS file for these parameters.

The different land-cover databases are listed and sorted using a sheetfile by sorting and ordering each attribute of land-cover 295 database to enumerate a layer of a data and give it the value of parameters. The order of the layers are not the same for Strickler and Curve Number. The Strickler values are provided by the state of art. The values of CN are mainly established by using USDA (1986).

The different land-cover databases, each containing diverse land-use attributes, are processed to derive hydraulic parameters 300 such as friction coefficients (Strickler values) and runoff generation parameter (Curve Number). These land-use attributes are systematically classified and organized within a table according to a predefined hierarchy of importance. In this hierarchical system, attributes are prioritized (the first attribute at the top, the last at the bottom), with higher-priority attributes determining the assigned parameter value in cases of overlap. It is important to note that the specific hierarchical classification and subsequent parameter assignment may differ for Strickler coefficients and CN. Strickler values are typically sourced from state-of-the-art literature or empirical studies, while CN values are primarily established using methods detailed in USDA 305 (1986). The correspondence table between land use and Curve Number values has been already shared with researchers or private companies and is available from the authors upon request.

The databases used vary between small-scale and national-scale applications, depending on the availability of each dataset.

The list below shows different databases used by decreasing quality (in terms of original resolution and informative content) in cases presented after:

310

- Polygon vector file used for example in riverbed
- French BDTopo IGN, a french vector IGN database of land-use (water surface, buildings, road, vegetation) and their sub-definition as width of road, level to the ground, cemeteries, type of vegetation...



- World OpenStreetMap buildings)
- French Cadastral parcels
- 315 – French RPG geographic database used as a reference for Common Agricultural Policy (CAP) subsidies
- European Urban Atlas for a complement of roads
- French Local authorities land use model
- French Large-scale land-use as OCS GE
- European Corinne landcover
- 320 – etc.

Vector objects are rasterized at 1m resolution, and combined into a mosaic by retaining only the non-overlapping areas from each successive layer. For Curve-Number, CN resampling is offered at other resolutions (5 and 25m, for example), working with the S parameter of the SCS method. Roads from BDTopo are processed with multiple road widths, each assigned a different effective Strickler coefficient in the model.

### 325 3.5 Hydraulic structures (optionnal)

Many of 2D shallow water models and mesh software enable to take into account culvert and mesh constraint line. The two types of hydraulic structures can be only used in C2D with refined mesh.

As described in the T2D user manual, a culvert is described as a couple of points between which flow may occur, as a function of the respective water level at these points. A GIS database is needed with a polyline for each culvert associated with 330 attribute value of the width of the culvert, the heights of the construction and the levels at the inlet and outlet.

Mesh constraint lines must be provided as a GIS database and are discretized with a spacing smaller than  $ds_1 = 3m$ . Currently, their elevation (Z) must either be directly represented in the DTM or manually incorporated if not captured—such as in the case of narrow flood walls, urban furniture, reinforced concrete guardrails (GBA), levees, canals, or other small-scale topographic features. These elements are often not fully represented in LiDAR-derived DTMs, which may filter out features like 335 table-like structures or lack bathymetric detail in minor riverbeds. However, their omission is generally more or less critical, depending on the modeling objectives.

### 3.6 Transect for discharge computation (optionnal)

As described in the T2D UserManual, a control section in T2D offers the possibility of obtaining the instantaneous flow rates through a specific segment of the domain. Segment means a polyline with only two points. Control sections are stored in a 340 specific database that serves as input for C2D, with only those located within each subdomain being utilized in the computation. The initial fortran routine of T2D stores the discharges and has been modified to store water depth and hydraulic head and was

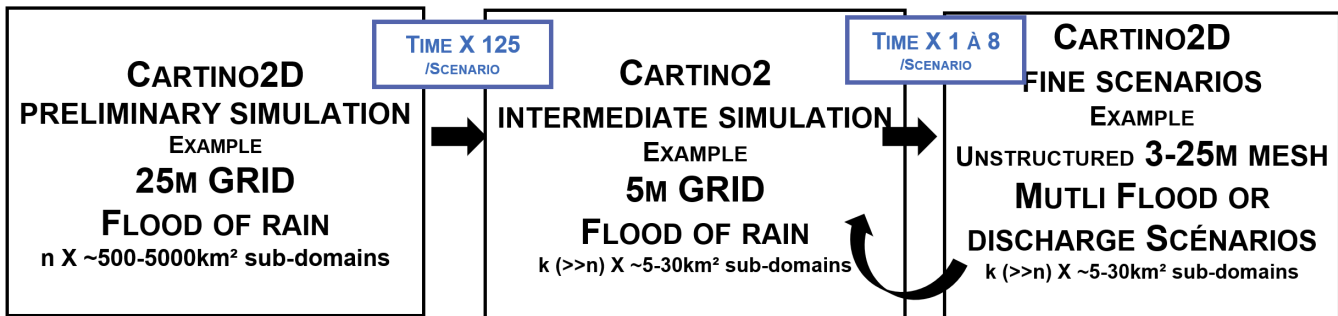


**Figure 10.** Automatic Domain sectorisation process with multi-resolution simulations

explained in Hocini and Pons (2024) and freely available on the development branch named MUFFINS in the OpenTelemac GitLab repository.

### 3.7 Automatic domain sectorisation process from multi-scale simulation

345 The interest of the meshing-simulation processes presented earlier is to largely remove the time-consuming aspect of mesh generation for hydraulic models and to quickly re-run calculations if databases are updated. However, this procedure requires a priori knowledge of reliable limits of our calculation zones, both for rainfall subdomains (well-defined watershed boundaries) and discharge subdomains (encompassing the entire floodplain). These limits may be known from existing delineations but not necessarily.

350 An optional sectorization strategy is proposed, which involves dividing the territory into independent subdomains. This strategy is beneficial for two primary reasons:

- **Hydrological Accounting:** It allows for the assumption of spatially uniform rainfall statistics over small subdomains, where neglecting spatial variability is a reasonable hypothesis.
- **Numerical Efficiency:** For numerical simulations, processing numerous small subdomains is generally less CPU-355 intensive than working on a single large domain within our modeling chain.

This sectorization approach is based on preliminary hydraulic simulations conducted over coarser regular meshes, progressing from an initial resolution of 25m to an intermediate resolution of 5m. This process is summarized in Fig. 10, with further details provided in Appendix A.

360 In summary, a calculation with a 25-meter step is conducted to highlight the main flow patterns. This calculation generates discharge sectors for finer mesh simulations by analyzing the time of the peak water height relative to the time of the peak rainfall. The greater the time difference between the peak water height and the peak rainfall, the more likely it is to be dealing with established watercourses. At the opposite, the smaller the time difference is, the more likely it is to be in the upstream parts of watersheds, and thus more likely to be dealing with rainfall sectors. With these assumptions, the delineation of the



5-meter discharge sectors is straightforward. The delineation of the 5m rainfall sectors is more complex and requires cross-  
365 referencing the affected areas with watershed footprints calculated from a DEM with modifications explained in Appendix A. The transition to the unstructured grid is achieved using the same sectorization; the dense unstructured mesh is established based on the results from the 5-meter step.

#### 4 Illustration Cases presented

To demonstrate the versatility and applicability of the C2D model, we have selected several test subdomains across France,  
370 including both the hexagonal mainland and overseas territories. Among these, two particularly extreme cases are presented, with a detailed focus on firefighter interventions in the third case (Pons and Hocini, 2025):

- A nationwide calculation case at the scale of France, demonstrating a preliminary application of the C2D model.
- A more localized calculation case, typical of C2D studies, which includes the integration of numerous hydraulic structures using unstructured meshes.
- 375 – An in-depth focus on Grabels city, a small catchment area, for the first comparative analysis with firefighter interventions.

##### 4.1 Nationwide Implementation in France

The General Directorate for Risk Prevention (DGPR) of the French Ministry in charge of ecological transition aims to establish a 'national flood map' accessible to services and the public. The objective set by the DGPR is indeed to develop and publish on the Géorisques website, for the benefit of citizens, an initial map providing information on whether any subdomain of the  
380 national territory (Hexagone and overseas) is flood-prone or not, for a flood event (due to overflow or runoff) with a return period of around 100 years. This work is included in the plan France Adapts Living at +4°C (PNACC) axis 1 - measure 3).

**The results of this national implementation, although preliminary findings are encouraging, have not yet been published and are currently undergoing local evaluation. This evaluation aims to identify significant limitations and anomalies in this work. The examples and illustrations provided in this article are for indicative purposes only and should not, 385 under any circumstances, be considered as final results.**

The principle for creating this map involves establishing a patchwork of the footprints of various flood hazard maps as:

- National existing knowledge:
  - Flood Risk Natural Prevention Plans (PPRi) (Hazard maps if possible, regulatory zoning otherwise),
  - Hazard maps (Flooding runoff and/or runoffs), subject to a "Porter à Connaissance",
- 390 – And a 'base map', as approximate envelopes of floods with a medium probability (Carte Socle in french):
  - Produced over the entire national territory (but displayed only on configurations not covered by local knowledge) with C2D, a Digital Terrain Model (DTM IGN) at 25 meters, with SHYREG rain and discharge (T = 100 years).



Thus, the map produced through C2D modeling is proposed to fill all the territories not covered by previous flood areas. The process of C2D was used at a preliminary scale (25m) using SHYREG statistical rainfall for a return period of 100 years.

395 The case quickly presented in this article is the "100 years" return period scenario. The topography used in this study is compiled from the most extensive available Lidar DTM data in France, covering more than 450,000 km<sup>2</sup> at a resolution of 0.5 or 1 m. The other part of the territory is covered by a DTM of 1m resolution with less elevation accuracy. The Lidar topography data of all the bordering countries has been collected freely on the web and converted to the french projection and elevation. A 25m DTM has been created by tile of 1 square kilometers. A 25-meter resolution Curve Number (CN) raster, employing the 400 same 1 km<sup>2</sup> tiling scheme, was also generated using the BDTopo database (IGN), the graphical parcel registry linked to the common agricultural policy (French CAP data) and CLC as explained in Section 3.4. 95 layers or selections into layers are done to perform 22 values of curve number in the range of 70 to 100. The Strickler friction coefficients are set to a constant value of 25m<sup>1/3</sup>/s for wetted surfaces(based on IGN BDTopo database), and 15m<sup>1/3</sup>/s elsewhere.

405 For rain and discharge sectorization at the french scale, an automatic sectorization is tested as presented in Section 3.7, and appendixA. A C2D simulation using a 100m DTM, chosen for its applicability to very large domains (as opposed to a 25m DTM), gave unsatisfactory results. This 100m DTM significantly restricted hydraulic flow, leading to inconsistent outcomes, particularly in very flat areas.

For this purpose, the rain and discharge sectorizations at french scale were established with varying degrees of manual intervention using:

410

- The watershed delineations of hydrographic sub-subdomains from the (SANDRE database)
- Two flood prone areas developed in the first french preliminary flood prone assessment (European Flood Directive)
  - The maximum "natural" flood prone areas (called EAIP in french), a by-product of the Preliminary Flood Risk Assessment (2011)
  - The Exzeco 25m data (2011) used for the production of the EAIP using Exzeco method (Pons et al., 2010)

415 The decomposition leads to 244 rainfall subdomains and 10 discharge subdomains (Fig. 11). Rainfall domains are forced by a spatially uniform statistical rainfall. Normally, this type of approach must take into account a spatial reduction of rainfall when dealing with large areas. We don't process to a spatial reduction to have maximal runoff and flood areas on upstream part of all the watershed. For the two types of subdomain, C2D and T2D are used. and the associated results by rain or discharge approach are merged. The same work has be done on french overseas territories and lead to have 271 C2D-rain sector. For 420 overseas territories, sectors were the entire islands. (Fig.11).

For this case, two hundred rainfall subdomains was totally processed at the first T2D calculation, 44 subdomains have to be modified manually with (1) small modifications as decrease time step for mountains subdomains or (2) increase duration for very flat subdomain, and (3) with hard modifications such as changing contour shape or some parameters as the Topographic Modification  $dZ$  (Section 3.1.1) reduced sometimes at 1m on very flat areas to limit the number of flux boundaries.

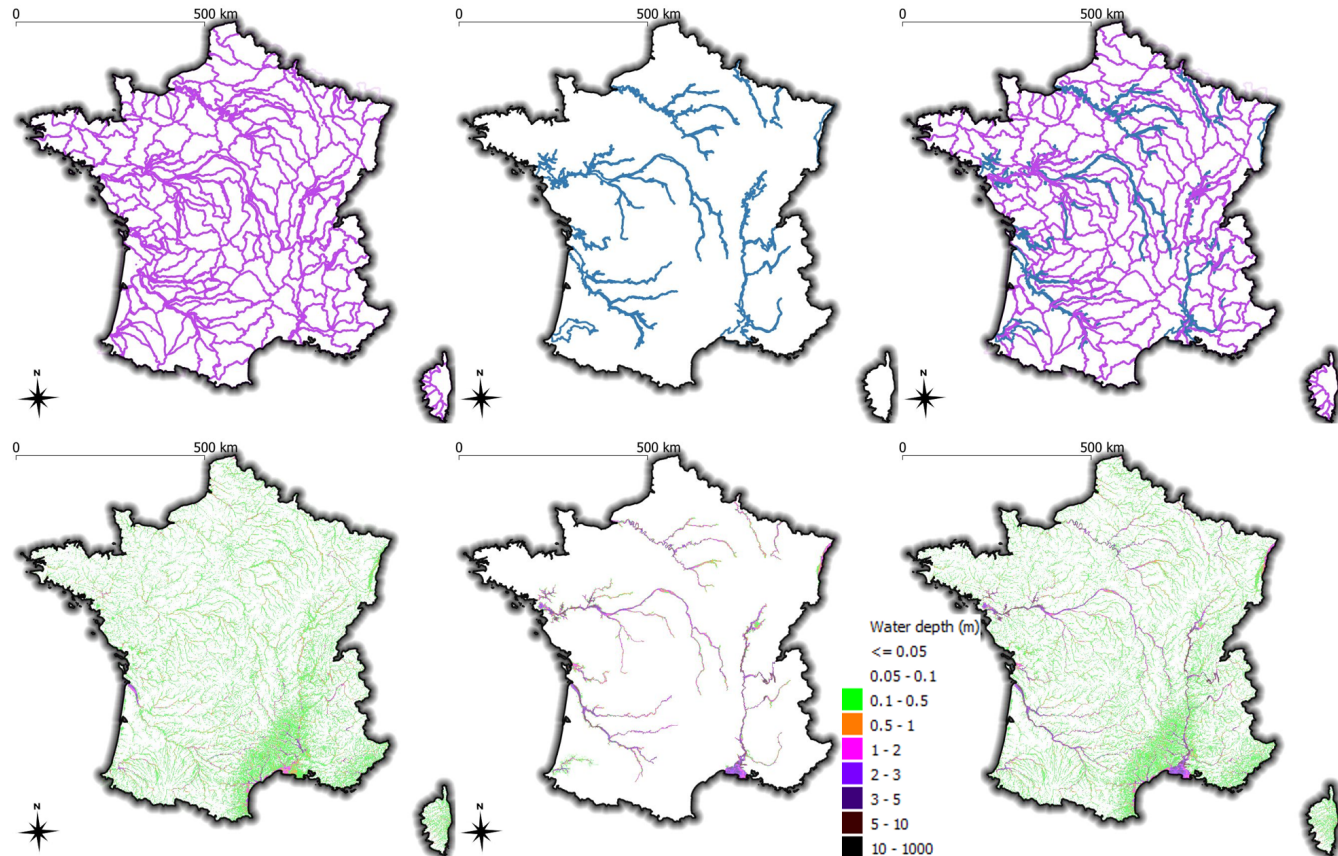


**Figure 11.** Nationwide flood-inundation map simulated with Cartino2D at 25m resolution on a structured grid. Hydrological forcing applied via C2D-Rain for upstream catchments and C2D-Discharge elsewhere, driven by SHYREG 100-year return period rainfall or discharge. Panels from left to right represent: rainfall-driven sectors, discharge-driven sectors, and combined forcing. Top sub-panels indicate sector boundaries; bottom sub-panels display resulting water depth distributions.

425 **Computational time.** The 244 C2D-Rain (resp. 10 C2D-Discharge) subdomains—each with a mesh containing up to 13,250,000 (resp. 10,750,000) cells—are run in parallel using the T2D hydraulic solver. Depending on the subdomain, the physical time period simulated is between one and twenty days long. Computations were distributed across various computing architectures, ranging from CEREMA HPC, as well as the GENCI national HPC infrastructure, utilizing between a few to 512 CPU nodes. The overall computation time was approximately three weeks for C2D-Rain and one week for C2D-Discharge.

430

An example of the C2D-Rain result is available on south of france (Fig. 12) for a 100y return period forcing. For each sector, C2D can provide high water depths, high scalar flood rate, etc. Two kinds of data enables to assess the process and evaluate or compare to local knowledge.

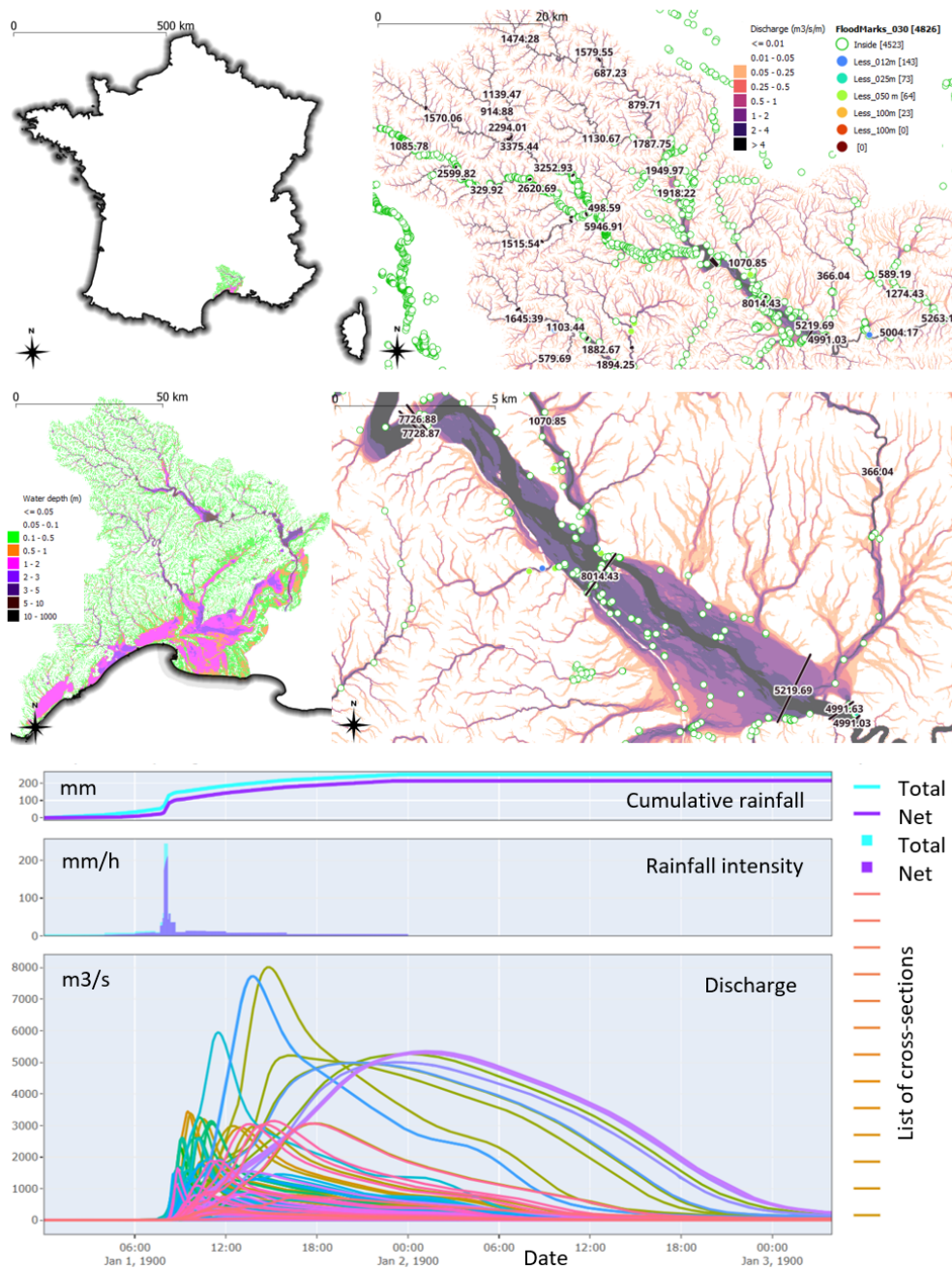


**Figure 12.** Top: Zoom-in on the upstream catchments of the Gardon rivers. Displayed elements include: simulated high water depths, lineic discharge (i.e., "high scalar flood rate" in Telemac 2D,  $m^3/s/m$ ), and the comparison between simulated flood extents and the planimetric positions of historical flood marks (from various past events, sourced from the French national database; floodmark score calculated by administrative department). Also shown are discharge values ( $m^3/s$ , in black text). Bottom: Time series of rainfall volume (top panel), rainfall intensity (middle panel), and simulated discharges at control sections (corresponding to the black text values shown on the maps).



435 – Cross-sections. We create almost 8000 control sections in france. For that C2D-rainfall sector of 6147 km<sup>2</sup>, 101 control sections re used. T2D gives us a lot of hydrogram (12). The high value of each hydrogramm is located on the maps. In this case, 8000 m3/s are in Gardon enque Plain before the canyon of "Gorges du Gardon" crossed at the end by the ancient Roman aqueduct "Pont du Gard". The plain of Gardon enque, located upstream from the Gorges du Gardon, has an important impact on flood attenuation and peak flow reduction. The value of peak discharge are 8000 m3/s before the "Gorges" and 5000 inside the "Gorges". This value are on the range of the value proposed in (Sheffer et al., 2008).  
440 According to the authors "at least three floods were bracketed by discharges between 6850 and 7100 m3 s- 1, and at least two floods reached a magnitude above 8000 m3 s- 1. Therefore, the extraordinary flood of 2002 was not the largest in the basin, estimated values of the 2002 flood was 6600 m3/s in the canyon." The values of 5000 and 8000 m3/s are in the range.

445 – There is a good visible agreement between the results and the floodmarks available on the (National Floodmarks Collaborative Platform). The position of floodmarks is analyzed to know if floodmarks are inside or outside our flood prone area. In that case "outside", the distance to the flood prone area is given. On the french department of Gard (number 30), the legend enables to see that on 4826 floodmarks available, 4523 are within our results and 143, 73, 64, 23 are respectively within less than 12, 25, 50, 100 meters. A national view of this analysis is given Fig.13. The main part of floodmarks are within our results (58057), while 2211, 1109, 823, 385, and 99 are respectively within less than 12m, 25m, 50m, 100m, or beyond 100m. These data provide an initial idea of the 'completeness' of the identification of flood-prone areas. It is logical that some markers are outside the base map, for example, if they correspond to events exceeding the centennial level or if they correspond to measurements in areas subject to solid transport or related to debris jams."

## 4.2 Aix-Marseille Provence Metropole area

455 An experimentation to build complex flood inundation indicators in semi-automatic hydraulic modeling has been applied to the numerous small watersheds of the Aix-Marseille-Provence Metropolitan area (MAMP).

Building on the results of recent research project (French ANR PICS and ANR MUFFINS), the aim is to experiment with semi-automatic hydraulic modeling on a large number of small watercourses, taking into account complex indicators such as urbanization, de-impermeabilization, hydrometeorological thresholds, and the evolution of soil physical properties due to climate change. Its purpose is to establish a homogeneous, evolving, and dynamic atlas of flood hazards for the small watersheds 460 of MAMP. This work will provide new insights into runoff risk (convention).

C2D-Rain method has been used at the three levels, preliminary (25m), intermediate (5m) and fine (unstructured 3- 25m), described in Figures 10 and A1. The division into two zones: rain and discharge are shown in Fig. 14. On the one hand, the rain sectors are defined to have a peak water height less than 1 hour after the rainfall peak. On the other hand, the discharge sectors are defined to have the peak of water depths more than 45 minutes after the rain peak. The simulation is done with a 465 the record of rainfalls recorded by Météo France on the french Mediterranean region.

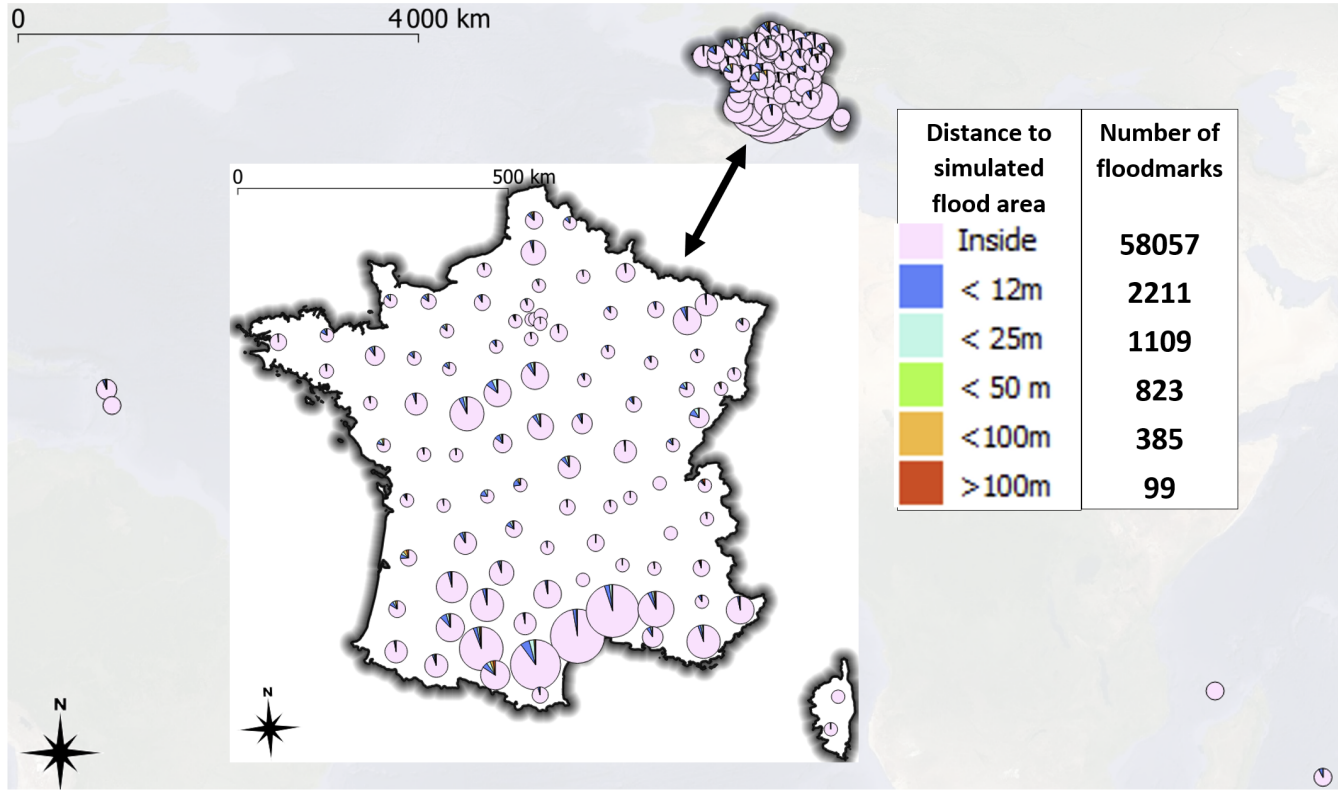


**Figure 13.** Comparison of simulated flood extents (100-year SHYREG statistical forcing) with historical floodmarks from various past events, sourced from the French national database. Simulations are centered on the centroid of each French administrative department (metropolitan and overseas), represented in hexagonal layout. Nearly 90% of recorded floodmarks fall within the simulated inundation areas. The number of floodmarks per department is indicated in parentheses in the legend. Background image source: Google Maps, © 2025 Google.. .

For the first steps, we focuses on the southern part of the metropolis (Fig. 15 bottom right) to develop and test methods to manage hydraulic structures. Cloud IGN LidarHD classification enables to have different kinds of classes, and the most important for our method is the ground and the bridges. Even if classification is more than 95 or 99 % correct (done with AI and human work), detailed hydraulic simulations are very dependent about the quality of small and big hydraulic structures.

470 We defined two kinds of hydraulic structures (Figure. 15)

– **Underground hydraulic structures.** These structures are "small structures" such as culverts, pipes in a lot of infrastructure embankments. It is very difficult to know all these hydraulic structures on territories. We use three types of information to create our database:

- Analysis of **depressions** which can be done everywhere depending only on the DTM accuracy
- **Potential bridge zone**, (Section 3.7 and Appendix. A)

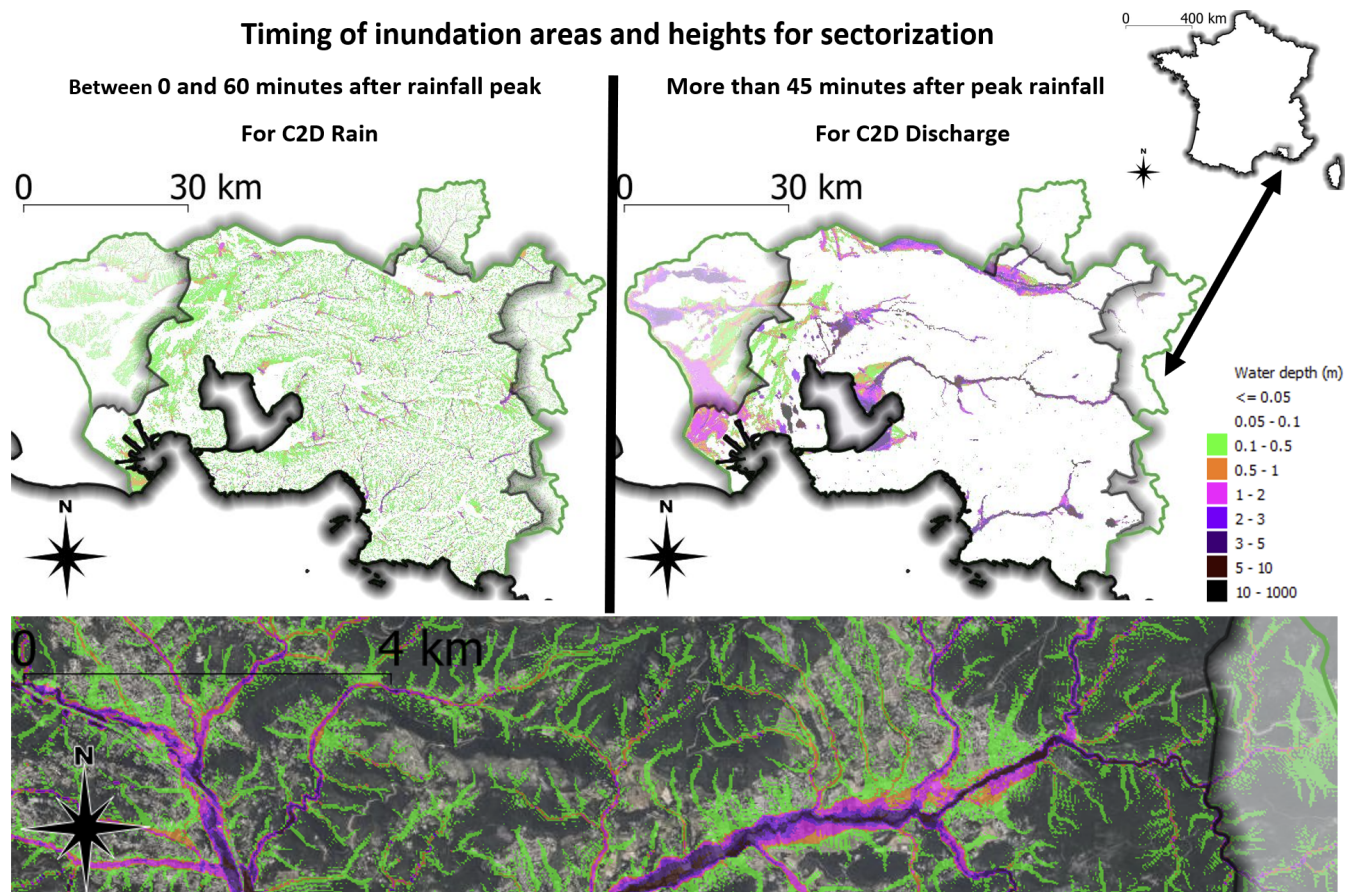


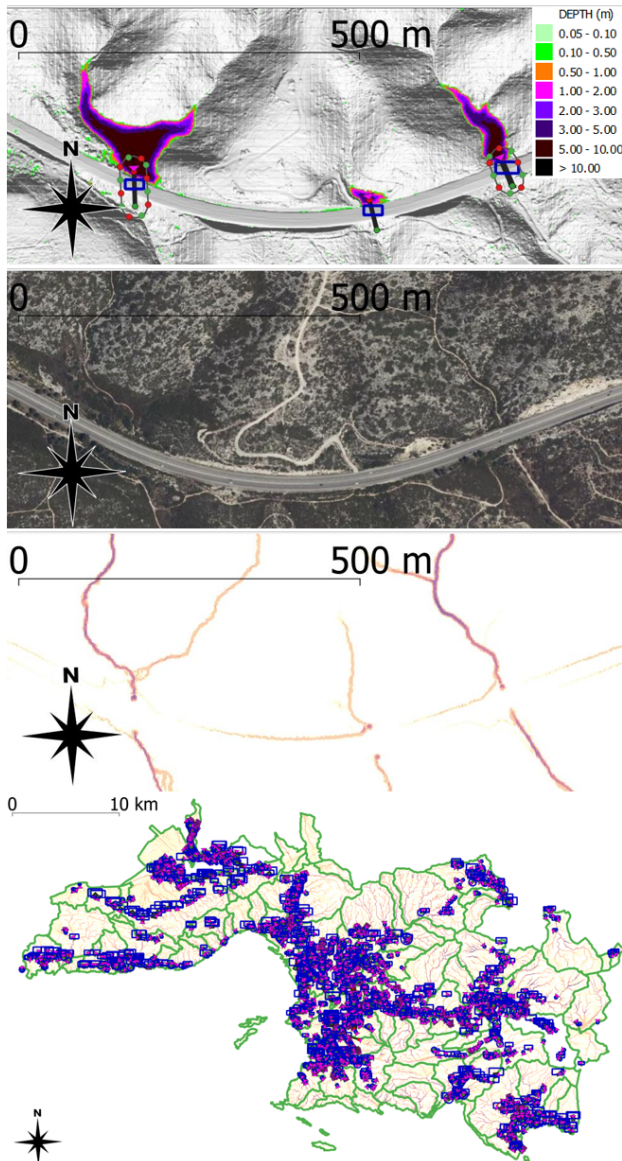
**Figure 14.** Example of hydrodynamic considerations for sectorization in C2D. The domain is split into upstream and downstream catchments: in upstream areas, there is a small lag between the rainfall peak and the simulated discharge peak; in downstream catchments, the lag is more significant. The figure illustrates rainfall and discharge areas as linked to the temporal analysis of peak flow (top), and shows a 25m resolution modeling result (bottom). Background image source: Ortho IGN, ©IGN.

- **Local hydraulic structure database** in different formats provided by infrastructure managers (road, rail, water-courses)

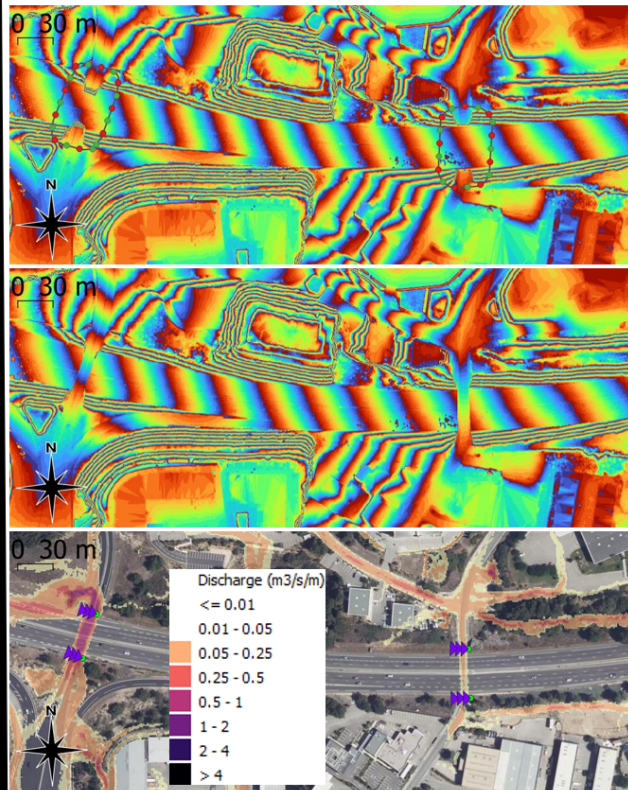
Any of the three approaches is complete. It is necessary to cross information to know if there is a potential culvert/pipe. Depressions are well adapted in the "rural" areas, to detect some blockage of infrastructures. Potential bridge zones are also interesting but not completed as shown in the Fig. 15. In urban areas, numerous underground structures may be present, making access to local databases essential. To optimize manual effort, we frequently rely on the OHFLASH Qgis plugin to efficiently cross-check and analyze various datasets. Through such underground structures—such as culverts or stormwater pipes—water can flow in pressurized conditions rather than as free-surface flow described by the shallow water model.



### Underground hydraulic infrastructures



### Infrastructure underpasses



	Potential bridge zone
	Culverts
	Cross-section to open DTM

**Figure 15.** Management of hydraulics Structures - Underground structures (left). DTM, Depressions, Potential bridge zone and culverts (top left), Orthophoto IGN (middle-top left), Scalar flood rate with no surface water on culverts (middle-bottom left), Visualization of more than 5000 underground hydraulic structures on 800 km<sup>2</sup> (bottom left), Infrastructure underpasses (left) DTM in cycling colors each 0.1 meter (right), top DTM without cleaning road underpasses, above with manual correction, result with flow in 2d shallow water in infrastructure underpasses. Background image source: Ortho IGN, ©IGN.



485 – **Infrastructure underpasses.** When two infrastructures intersect, the passage of the lower infrastructure is physically restored but can not be present in Lidar DTM. To manage this infrastructure underpasses, we have the possibility to create a cross-section on each side of the upper infrastructure and interpolate between two cross-sections. The DTM is modified and the hydraulic simulation show the flow throw this path.

490 The crucial question for the local simulation is "What is the ground". We explain two types of hydraulic infrastructure management, but the limit between the two approaches is sometimes blurred. So it is also complex to know the limit between an integrated underground structure or open bridges.

In the south parts of MAMP, more than 5000 underground hydraulic infrastructures were integrated and this number don't take into account most of the hydraulic structures with a dimension less than 800 mm of diameter. We also create more than 450 cross sections to "open" the DTM.

495 For these 800km<sup>2</sup>, with 90 rainfall C2D sectors, C2D enables to create quickly and replay several time T2D to manage numerous adjustments for hydraulic structures by an iterative approach, simulation, check, modifications.

On these area, in situ measurement of underground hydraulic infrastructures are in progress to complete the C2D simulations. The evaluation of the simulations on very small catchments will be done with some few gauge stations but mainly with the analysis of firefighters interventions.

500 In a synthesis about hydraulic structures, each modeler in each case has to cope with a dilemma about what is the ground and what is not the ground. The choice between inserting or not a underground structure into a model or open the DTM could also depend on the 2D models used, some are more efficient for one solution or the other.

### 4.3 Grabels city

505 On the night of October 6-7, 2014, the commune of Grabels, located north of Montpellier, experienced an extreme rainfall event characterized by intense and stationary storm cells. This event resulted in significant flooding.

The episode was marked by exceptionally heavy rainfall, with up to 250 mm recorded in just some hours over the northern part of Montpellier, including Grabels (Fig. 7).

510 The intense rainfall caused major flooding in the Mosson and Lez watersheds. Grabels was particularly affected, with parts of the city submerged by the Rieu Massel, a small tributary of the Mosson River ( $\simeq 5\text{km}^2$  catchment). The flooding resulted in considerable damage and disruptions, including overturned vehicles due to the flash floods.

The sector of Grabels was studied and presented in Fig.1, Fig.3, Fig.4, Fig.5, Fig.7 and Fig.9.

Regarding these types of intense runoff and flash flood events, data to assess the consistency of simulations are often limited. In Grabels, flood marks are available but are located in the downstream areas and only provide the maximum levels without their timing, hence no information on flood-inundation dynamics. We also had access to damage reports (which are not publishable). 515 To better analyze our simulations, we obtained access to firefighter interventions, which allow for another approach to dynamic evaluation.

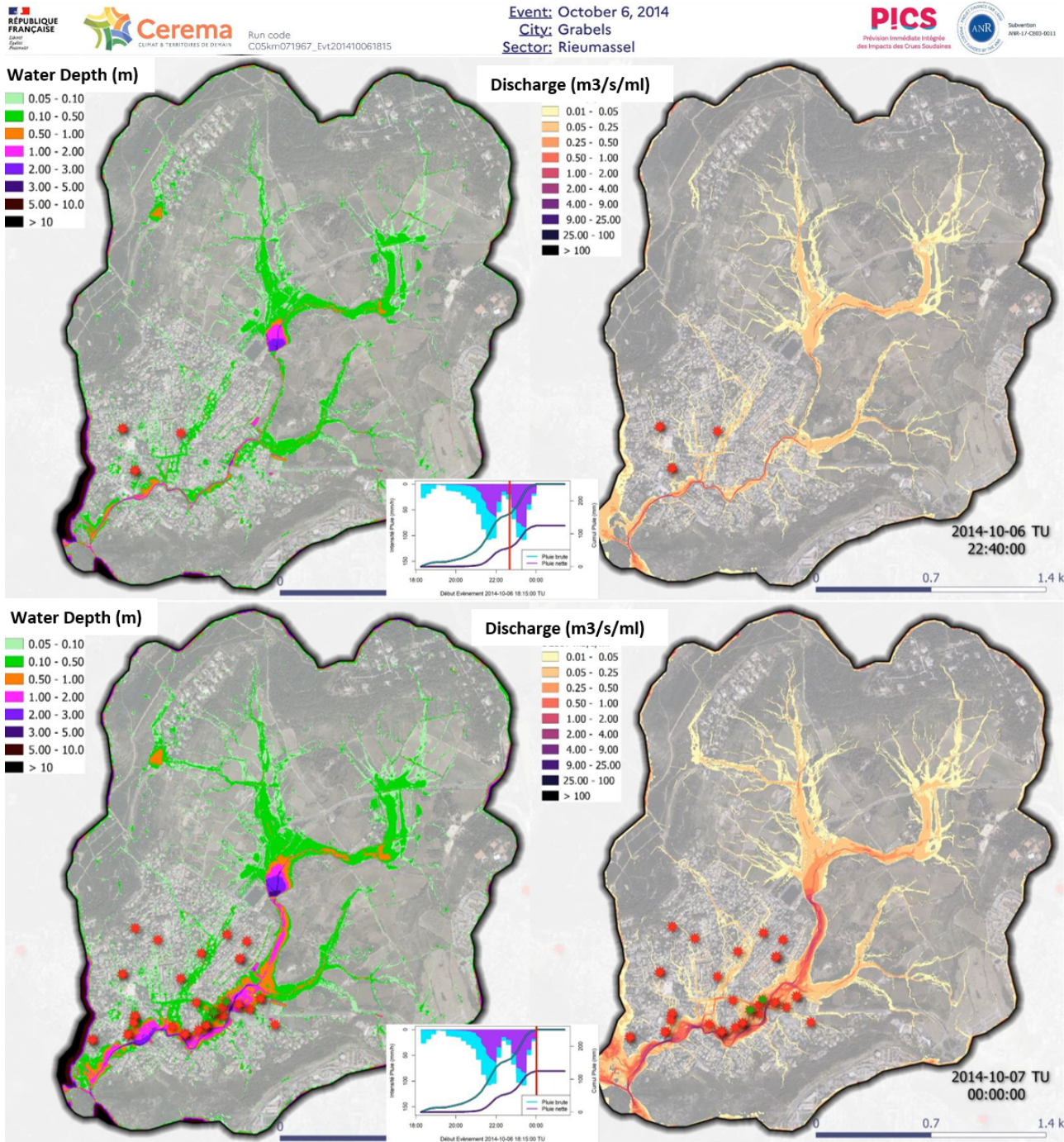


**Figure 16.** Comparison between the replay of the rainfall event from October 6-7, 2014, and firefighter interventions, with video captures at 10/06/2014 10:40 PM (top) and 10/07/2014 00:00 AM (bottom). The stars represent the timestamped firefighter interventions. The hyetograph shows raw rainfall in cyan and effective rainfall in magenta; the red line on the hyetograph indicates the timeline. Background image source: Ortho IGN, ©IGN.



Firefighters maintain logs that record the times when individuals call for help. By creating videos of simulations and visualizing them with timestamp management, firefighter interventions can be analyzed to determine if hydrological-hydraulic model outputs and flow patterns are consistent with the calls location and timing (Fig.16).

520 In the video captures of this event simulation, three stars appear at 10/06/2014 10:40 PM (top), and the stars are not primarily located in the main channel of the very small Rieu-Massel "river"/"thalwegs" but in sectors affected by heavy rain triggering runoff as simulated. By 10/07/2014 00:00 AM, many stars appear, and their concentration is more closely linked to the main path of the flood pattern. This analysis, though only visual and subjective, helps to demonstrate the relative efficiency of the 2D hydraulic model with SCS-CN method for net rainfall determination.

525 The two captures illustrates the following: If runoff occurs too early, calls to firefighters appear before the flash flood. If the calls are too late, the flash flood has already passed before the calls are made.

The graphic at the bottom and in the middle of the video captures shows raw rainfall in cyan and effective rainfall in magenta. This allows us to represent soil saturation and its impact on effective rainfall. The second, shorter peak of rainfall, with the same intensity as the raw rainfall, is much more significant in terms of net rainfall.

530 Currently, this analysis is only visual. It is difficult to provide statistical analyses for various points:

- Each emergency service (mainly named SDIS in France) currently utilizes its own tools, databases, and naming conventions for interventions specific to its territory.
- The location of an intervention is typically based on an address. However, the precision of this localization can vary. In most cases, the intervention location is tied to the address of a property. The recorded position of the address can vary based on the database used; it might correspond to the mailbox, the centroid of the building itself, or the centroid of the parcel. Depending on the parcel's size, the centroid might fall completely outside the flooded area.
- In some instances, the location of an intervention is not a specific building but rather a neighborhood. This is particularly common during major events where firefighters conduct reconnaissance of all houses.
- Interventions can encompass a mix of emergency calls from citizens and pre-positioned intervention units or advanced command posts.

540 Despite these limitations, these elements seem very useful to analyze in the context of very small, ungauged watersheds where little information and few measurements are easily collectible.

## 5 Conclusions and perspectives

This study presented Cartino2D (C2D), a novel automated framework that enables the deployment of a 2D shallow water with 545 rain and infiltration, here the well established Telemac2D model (T2D), over very large domains, with flexible hydrological forcing—either by rainfall or discharge hydrographs. The framework integrates unstructured mesh generation, topography-based refinement, and incorporation or determination of hydrological and hydraulic parameters from geospatial datasets, allowing multi-resolution simulations up to very high metric resolution.



After a detailed explanation of the different steps of the framework, it has been successfully applied and showcased at country scale over France, and at very high resolution in complex urban areas such as the Marseille Metropolitan area and a zoom on Grabels city. Model outputs were evaluated using available flood marks and firefighter intervention records. Preliminary results show promising consistency, although they highlight sensitivity to parameter selection and the challenge of calibrating high-dimensional hydrological–hydraulic systems. The statistical discharge values from SHYREG, although hydrologically calibrated, can show significant mismatches when compared to high-resolution simulated flows—underscoring the need for integrated calibration and the development of spatial rainfall generators for more realistic scenarios. This represents very interesting perspectives that will be investigated in further research.

Several technical aspects were identified for improvement, including the representation of culverts within T2D, an improvement of the number of antecedent moisture condition of SCS-CN infiltration models, and the evaluation of alternative infiltration models such as Green–Ampt. The objective is also to adapt the framework for developing real-time flood forecasting. The framework is also being extended to support coastal boundary conditions and sea surge modeling applications.

Looking forward, future work will also explore applicability with the use of freely available global high-resolution DEMs (existing or forthcoming ones with remote sensing improvements) and further test the generalization of C2D on international territories to assess its full potential for global-scale high-resolution flood inundation modeling.



## Appendix A: Details for the Automatic Domain sectorisation process from multi-scale simulation

565 A preliminary C2D calculation at 25m (C2D\_25m) is performed with heavy rainfall (return period >1000 years, meteorological records) over an extended subdomain (user defined) of up to a few thousand km<sup>2</sup>. The simulated water depth and lineic discharge, enables to define the so-called flood-prone areas based on thresholds:  $q > 0.1$  and  $h > 0.2$ , where  $q$  in [m<sup>2</sup>/s] is the scalar flowrate and  $h$  in [m] is the water depth. These thresholds are defined according to our experience with a 25m resolution. Then, the results of this C2D\_25m modeling enable to determine two types of contours: - Discharge contours for  
570 C2D\_Discharge\_5m - Rainfall contours for C2D\_Rain\_5m aiming consistent drainage area detection regarding hydrological-hydraulic connectivity Fig. A1.

To distinguish subdomains mainly affected by rainfall at the head of watersheds (flash floods) from subdomains mainly affected by river overflows, we rely on the time of the water height peak  $t_{peak,C2D\_25m}$  in the C2D\_25m modeling performed with a triangular rainfall hyetograph. In principle, the shorter the duration between the water height peak and the rainfall peak  
575  $t_{peak,rain}$ , the more it will correspond to a flash flood. Conversely, the longer the duration between the water height peak and the rainfall peak, the more it will be an area of established flows in small to large rivers that are more known and visible in the territory. The following two equations are therefore used:

$ZI_{riverflood}$  corresponds to  $q > 0.1 \text{ m}^2/\text{s}$  and  $h > 0.2 \text{ m}$  and  $t_{peak,C2D\_25m} > t_{peak,rain} + dt_{river}$

580  $ZI_{flashflood}$  corresponds to  $q > 0.1 \text{ m}^2/\text{s}$  and  $h > 0.2 \text{ m}$  and  $t_{peak,C2D\_25m} > t_{peak,rain} + dt_{flash}$

In southern France, the values of  $dt_{river}$  and  $dt_{flash}$  are taken, respectively, in 20/60 minutes and 25/75 minutes. Therefore, there will be overlaps between "flash" and "river" zones. This allows for some flexibility because the boundary between a flood zone and a flash zone is never clear-cut. These values defined a priori from fine scales considerations enable our discharge subdomains to be consistent with subdomains of the French flood forecasting system Vigicrue forecast  
585 (https://www.vigicrues.gouv.fr).

A discharge zone  $ZI_{riverflood}$  can be converted almost instantaneously into a Discharge subdomain for C2D-Discharge-5m. Some cleaning is necessary for small subdomains, but most of the time, only the very large surface areas need to be retained.

590 Defining Rainfall subdomains, on the other hand, requires other more laborious steps. The objective is to cross-reference a precise watershed delineation with  $ZI_{flashflood}$  to create Rainfall contours.

To achieve a precise watershed delineation using the classical flow direction algorithm (Jenson and Domingue, 1988; Tarboton, 1989), the DEM will be reprocessed with two procedures:

595 – **Depressions.** Work on major topographic depressions defined as areas with topographic hole in which storage volume is greater than the volume of a given rainfall such that:  $ZI_{megadepression}$  corresponds to  $h > 0.2 \text{ m}$  and  $t_{peak,C2D\_25m} = T_f$ , where  $T_f$  corresponds to the final time of the simulation. After automatic detection, a manual verification is done, for example with a proposed Qgis plugin called OH Flash), to retain the two first mega depressions types among those three that can appear:

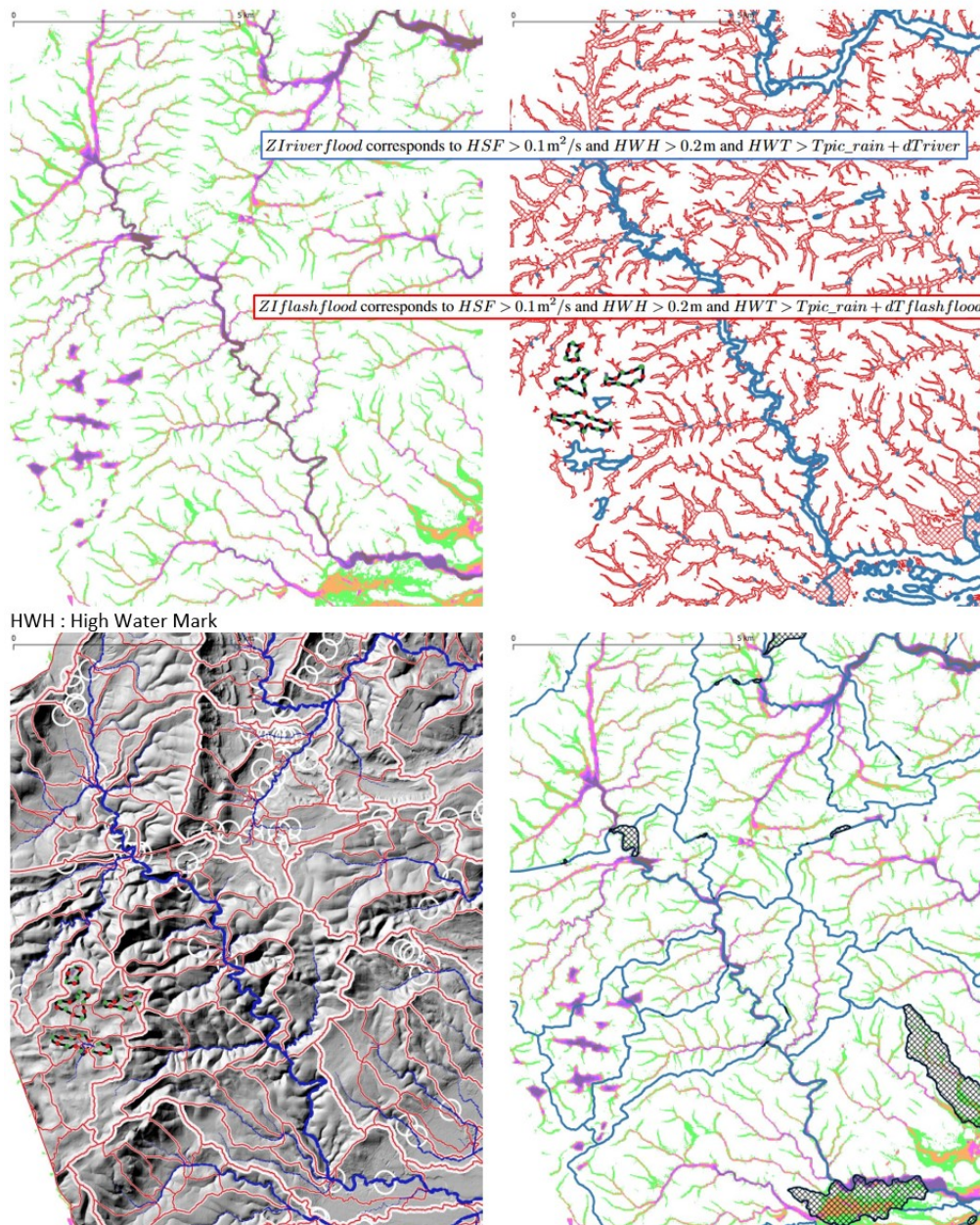


**Figure A1.** 25m high water level results (Top-left), Rain parts (red) and discharge sectorization for 5m next step (cyan) (top-right), Watershed (red line) and streamnet (cyan line) on a modified DTM (bottom left) including potential bridge zone and hole in huge depressions, Rainfall sectorization (cyan line) on the 25m results for the 5m step - gray-out areas correspond to overlaps rainfall subdomains



– (Retained) natural mega-depressions called polje, sinkhole in karstic areas,

– (Retained) human mega-depressions linked to some anthropic excavation of the ground as Quarries, Open-pit mines

600 – (Excluded) false mega-basins due to transport infrastructure embankments. It is not always easy to know if there is hydraulic restoration structures under road or rail infrastructures.

– **Potential Bridge Zones.** No stream burning is used to preserve LiDAR DEM richness and we prefer to lower elevation only in "potential bridge zones" (terminology introduced by french IGN) that can block flows at coarser resolutions. Potential bridge zones are derived from GIS processing based on existing databases in France (with no direct link to the DEM used) describing land use. The main database is the IGN BDTopo already mentioned (Section 3.4). Other non-publicly accessible point databases, such as the national road network or the concessioned national road network, are used. In the BDTopo, two types of objects coexist: surface objects and point objects. Without going into the details of each layer of the BDTopo, surface objects with attributes of the "Ponts" type in French (bridges) are retrieved. Road, rail, and water (rivers and canals) transport networks are mainly provided as linear objects with attribute fields giving an order of magnitude of the widths associated with these objects. The very useful field is the information about the position relative to the ground available for these three types of networks. An analysis is launched between all types of linear objects and their levels relative to the ground. For example, a hydrographic network at level -1 that intersects a road network at level 0 will be retrieved, and the footprint width of the overlap zone will come from approximate widths calculated with the attributes of each table. All surface objects derived directly from databases or intersections are then 610 merged. At the scale of France, 385000 objects are detected in France, i.e. 2 objects every 3 square kilometers.

615

Note that, for watershed delineation, the DEM for C2D\_25m can be used, but in practice, we prefer to work on a more precise DEM for downscaling to a 5m resolution, for example. This DEM is:

620 – masked with nodata around the low points of mega-basins (all points between the low point and an elevation delta, for example, 50 cm to 1 m),

– lowered in potential bridge zones with an arbitrary value of 25 m.

Finally, after removing depressions and potential bridge zones, an improved flow direction computation can be done with the D8 algorithm applied at the working resolution, using the TauDEM tool controlled in R.

625 Vectorial objects of watersheds and stream networks are created with different thresholds on drainage area. The lowest threshold of  $0.5 \text{ km}^2$  is used to determine the watersheds. A  $5 \text{ km}^2$  threshold on streamnet is used to split into left and right bank watersheds of  $0.5 \text{ km}^2$ , enabling to capture only rain parts.

Next, this step aims to treat overlaps in the obtained flood-prone area  $ZIflood$  and the splitted watersheds. For each object in  $ZIflood$  with an area greater than a threshold, for example,  $10,000 \text{ m}^2$ , the divided watersheds are merged. These merged watersheds constitute the Rainfall subdomains for C2D\_5m\_Rain. Some "orphan" basins are merged with neighbors (minimum rainfall subdomain, for example,  $2 \text{ km}^2$ ). This procedure generates duplicates that can be processed 630 in two C2D\_5m\_Rain subdomains. In practice, it is often interesting to keep these duplicates because the 5m calculation can



reveal real deflection zones on slopes or plateaus. The shapes of the subdomains are analyzed, mainly visually, to see if there are consistent. Modifications have often to be made but take less time than a manual work.

635 If the width of the flood discharge area is significant downstream rainfall sectors, it is advisable to merge the major bed part with the rainfall sectors to diminish the number of automatic boundary conditions and have a more stable boundary condition for the following steps.

Following this sectorization into C2D\_5m\_Discharge and C2D\_5m\_Rain, a C2D calculation with the parameters described in the section 3.1.1 is launched.

640 The results of C2D\_5m\_Discharge are analyzed to see if the extent of the valid zone is sufficient, as the transition from a 25m resolution to a 5m resolution can change a little bit the flow extents, sometimes with discharges not having quite the same orders of magnitude. A procedure is used to analyze the water levels reached at the boundaries with positive water heights to expand these zones in relation to the DEM. After these verifications, a calculation in unstructured mode is possible for C2D\_GMSH\_Discharge.

645 The results of C2D\_5m\_Rain are also analyzed, mainly visually, to see if the shape of the subdomains is consistent, analyse the stability of boundary conditions. Modifications can be made. The result of the flood-prone areas from this step, however, constitutes the basis for moving to an unstructured calculation in C2D\_GMSH\_Rain. The extent of the flood-prone area established from height and linear discharge thresholds (sometimes lower than those cited for a 25m resolution) is integrated to provide the construction points used as constraint lines for GMSH (redefined flood-prone areas cited previously).

650 The results of the unstructured C2D\_GMSH\_Rain are then analyzed. The sectorization can also be questioned. As with the 5m resolution, the shape of the subdomains is unlikely to need modification except if the integration of underground hydraulic structures fundamentally changes the flows.

In all the process, the polygonization of raster to vector is often preceded by work with positive and negative buffers on the raster and followed by work on smoothing vector data, removing small interior holes and small non-contiguous polygons.

## Appendix B: Precautions for use and limitations for nationwide Implementation in France

Precautions regarding the use of the base map is provided in the following non-exhaustive list of :

655 – The simulation resulting from a single-frequency hyetograph of a 100-year return period rainfall, or a peak flow of a 100-year return period, does not necessarily produce a mapping corresponding to a centenial event.

– Resampling at 25 meters tends to erase the effects of dikes, except for very large embankments.

– Resampling at 25 meters can lead to closing valleys or structural passages in embankments (or vice versa), resulting in modifications to certain flows (artificial dams, etc.).

660 – Hydraulic restoration structures in embankments (particularly infrastructure) and stormwater networks in urban areas are not taken into account (due to the absence of a precise database available at the national level).



665

- The calculation is done with "clear" water with Newtonian behavior; this work does not account for natural phenomena of solid transport, debris flows, lahars, blasts, bank or slope failures during morphogenic floods, floods caused by glacial or periglacial risks, or other types of "clear" water inputs such as snowmelt, spring resurgences, and rising water tables.
- This work does not consider natural or anthropogenic debris accumulations that can develop and break during flood events in natural or anthropogenic environments.
- This work does not consider the operations and functioning of dams and hydraulic weirs.
- This work does not consider dike breaches.
- This work does not consider breaches of anthropogenic dams.
- This work does not consider forced water flows such as pumping, hydraulic diversions, canal management, and water transfers.
- This work does not consider marine submersions, and the boundary conditions at sea are defined based on the current average level.
- The various databases used are also based on sizing calculation assumptions. Furthermore, some limitations are related to the lack of data available at national, regional, departmental, or even local levels.

675

The following additional limitations have also been identified:

680

- Flat areas tend to exhibit many more flow blockages around infrastructures, with the closure of hydraulic passages potentially completely blocking flows.
- Flow production in flat areas also seems to be low compared to the knowledge of these sectors. This weakness may be related to the previous issue or to runoff effects poorly represented by the SCS-CN approach. Surface flows can be supported by flows within soils.
- Vectorization can lead to a loss of flow continuity when transitioning from concentrated flow to diffuse flow in small tributaries or dry thalwegs. Vectorization can also group floodable areas of the main river course with floodable areas of tributaries parallel to this course, such as those from alluvial fans.



685 *Code and data availability.* FILINO, a tool for refining LiDAR data for flood analysis, is freely available at <https://github.com/CEREMA/filino> (last access: December 2025). FILINO is protected by the Agence pour la Protection des Programmes (APP).

OHFLASH, a QGIS plugin designed for verifying GIS data, is freely accessible via <https://github.com/CEREMA/OHFlash> (last access: December 2025).

690 The source code of Cartino2D is freely available on <https://github.com/CEREMA/cartino2d> (last access: December 2025). Cartino2D is also protected by the Agence pour la Protection des Programmes (APP).

To facilitate reproducibility, a dataset is provided to run Cartino2D v1.0, available in the GitHub repository above. This dataset includes all input data required to execute Cartino2D (see Section 3), as well as reference outputs for the two cases described in the article (see Figure 3 and Figure 12). These cases cover both a "coarse" 25m resolution and a finer resolution, with an overlap on Grabels areas. The dataset is permanently archived on Zenodo and accessible at <https://doi.org/10.5281/zenodo.17778608> (Pons and Hocini, 2025).

695 The upgraded TELEMAC-2D version with spatialized rainfall and other adaptations for Cartino2D is the MUFFINS branch, which is freely available in the OpenTelemac GitLab repository at <https://gitlab.pam-retd.fr/otm/telemac-mascaret/-/tree/muffins> (last access: December 2025).

The ANTILOPE J+1 product by Météo-France Champeaux et al. (2009) is a commercial product, and access is restricted to authorized users. An alternative product is available at <https://www.data.gouv.fr/datasets/reanalyses-comephore/>.

700 Access to the SHYREG statistical peak discharge database (<https://shyreg.pluie.recover.inrae.fr/>) and the SHYREG statistical rainfall database (<https://shyreg.recover.inrae.fr/>) requires prior authorization.

Regarding the nationwide flood map for France, the results presented are provisional. While the open-source code of Cartino2D, Filino, and the datasets used enable the reproduction of such maps, the current national flood maps cannot be redistributed due to an embargo related to administrative flood prevention plans and legal responsibilities. These maps will be partially integrated into local flood products 705 by the Directorate General for Risk Prevention (DGPR)—Ministry of Ecological Transition, Biodiversity, and International Negotiations on Climate and Nature.

For the nationwide case study, most Digital Terrain Models (DTMs) used are open-source, while a few require specific access agreements.

**– French DTMs are available on:**

- RGEALTI website
- LidarHD website

**– Foreign DTMs are available from the following sources:**



Country	Region	Reso (m)	EPSG	Shift used with French NGF	Links
Belgium	Flanders	1	31370	-1.73	<a href="https://www.vlaanderen.be/datavindplaats/catalogus/digitaal-hoogtemodel-vlaanderen-ii-dtm-raster-1-m">https://www.vlaanderen.be/datavindplaats/catalogus/digitaal-hoogtemodel-vlaanderen-ii-dtm-raster-1-m</a>
Belgium	Wallonia	1	3812	-1.77	<a href="https://geoportail.wallonie.be/catalogue/a004e570-99d6-4fe5-b83d-49b774409278.html">https://geoportail.wallonie.be/catalogue/a004e570-99d6-4fe5-b83d-49b774409278.html</a>
Luxembourg	Luxembourg	0.5	2169	0.56	<a href="https://data.public.lu/fr/datasets/lidar-2019-modele-numerique-de-terrain-mnt/#resources">https://data.public.lu/fr/datasets/lidar-2019-modele-numerique-de-terrain-mnt/#resources</a>
Germany	Rhineland-Palatinate	1	25832	0.53	<a href="https://www.sig-gr.eu/fr/outils-donnees/convention-echange-donnees/donnees-geographiques-rlp.html">https://www.sig-gr.eu/fr/outils-donnees/convention-echange-donnees/donnees-geographiques-rlp.html</a>
Germany	Saarland	1	25832	0.53	<a href="https://www.sig-gr.eu/fr/outils-donnees/convention-echange-donnees/donnees-geographiques-sarre.html">https://www.sig-gr.eu/fr/outils-donnees/convention-echange-donnees/donnees-geographiques-sarre.html</a>
Germany	Baden-Württemberg	1	25832	0.53	<a href="https://rips-metadaten.lubw.de/trefferanzeige?docuuuid=271f9e5b-6f12-4fc9-b692-cb7828e8c170">https://rips-metadaten.lubw.de/trefferanzeige?docuuuid=271f9e5b-6f12-4fc9-b692-cb7828e8c170</a>
Switzerland	Suisse	0.5	2056	0.28	<a href="https://viageo.ch/catalogue/donnee/300207">https://viageo.ch/catalogue/donnee/300207</a>
Spain	Zone 1	2	25830	0.04	<a href="https://centrodedescargas.cnig.es/CentroDescargas/catalogo.do?Serie=MDT02">https://centrodedescargas.cnig.es/CentroDescargas/catalogo.do?Serie=MDT02</a>
Spain	Zone 2	2	25831	-0.03	<a href="https://centrodedescargas.cnig.es/CentroDescargas/catalogo.do?Serie=MDT03">https://centrodedescargas.cnig.es/CentroDescargas/catalogo.do?Serie=MDT03</a>
Spain	Zone 3	5	25830	-0.04	<a href="https://centrodedescargas.cnig.es/CentroDescargas/catalogo.do?Serie=MDT04">https://centrodedescargas.cnig.es/CentroDescargas/catalogo.do?Serie=MDT04</a>
Spain	Zone 4	5	25831	-0.04	<a href="https://centrodedescargas.cnig.es/CentroDescargas/catalogo.do?Serie=MDT05">https://centrodedescargas.cnig.es/CentroDescargas/catalogo.do?Serie=MDT05</a>

Dissemination of the results presented for the national map and the Aix Marseille Provence metropolis is a shared responsibility, evaluated on a case-by-case basis between Cerema and the project owners.

715 Some results of the C2D\_GMSH\_Rain at fine resolution are available online at this link PAC Montpellier.

*Author contributions.* FP: Conceptualization, Methodology, Data Curation, Investigation, Formal analysis, Software, Writing - Original Draft, Visualization, Supervision, Funding acquisition, Validation, Project administration. NH : Software, Methodology, Visualization, Investigation, Validation, Writing - Original Draft. PAG: Writing - Original Draft, Conceptualization, Visualization, Funding acquisition

*Competing interests.* The authors declare that they have no competing interests



## 720 Acknowledgements

We would like to express our gratitude for technical exchange to Toulon Provence Méditerranée Metropolis, Vistre-Vistrenque river Basin Joint Authority (EPTB), Nîmes Metropolis, the City of Nîmes, Metropolis "Aix-Marseille Provence", the Community of Communes of the Gulf of Saint-Tropez, Asse-Bléone River Basin Joint Authority (Syndicat mixte), Departmental Directorate of Territories and the Sea of Hérault, Departmental Directorate of Territories and the Sea of Alpes-Maritimes, the 725 General Directorate for Risk Prevention of the french Ministry in charge of ecological transition, partners of the ANR PICS (ANR-17-CE03-0011) and partners of the ANR MUFFINS (ANR-21-CE04-0021) for their financial support in the technical development of the Cartino2D method.

We also extend our thanks for the supply of computing resources to IFREMER (for access to HPC resources), and GENCI for TGCC allocations (AD012A14287, AD012A14287R1, and AD012A14287R2).

730 Additionally, we would like to thank IGN for the Lidar programs, particularly the LidarHD program and their databases, INRAE for the SHYREG databases and Météo France for the rainfall datasets.

Mistral AI and ChatGPT were used for english revisions and improvements.

*Financial support.* All the organizations cited in Section B provided funding for the use of Cartino2D.

We also extend our thanks for the funding of equipment and the provision of computing resources to Predict Services with financing 735 from the ESA Cosparin project), Metropolis "Aix-Marseille Provence", the General Directorate for Risk Prevention of the french Ministry in charge of ecological transition, the ANR PICS and ANR MUFFINS projects, IFREMER (for access to HPC resources), and GENCI for TGCC allocations (AD012A14287, AD012A14287R1, and AD012A14287R2).



## References

Aubert, Y., Arnaud, P., Ribstein, P., and Fine, J.-A.: La méthode SHYREG débit—application sur 1605 bassins versants en France métropolitaine, *Hydrological Sciences Journal*, 59, 993–1005, <https://doi.org/10.1080/02626667.2014.902061>, 2014.

Bates, P. D., Horritt, M. S., and Fewtrell, T. J.: A simple inertial formulation of the shallow water equations for efficient two-dimensional flood inundation modelling, *Journal of Hydrology*, 387, 33–45, <https://doi.org/10.1016/j.jhydrol.2010.03.027>, 2010.

Champeaux, J.-L., Dupuy, P., Laurantin, O., Soulan, I., Tabary, P., and Soubeyroux, J.-M.: Les mesures de précipitations et l'estimation des lames d'eau à Météo-France : état de l'art et perspectives, *La Houille Blanche*, 95, 28–34, <https://doi.org/10.1051/lhb/2009052>, 2009.

contributors, G.: GDAL/OGR Geospatial Data Abstraction software Library, Open Source Geospatial Foundation, <https://doi.org/10.5281/zenodo.5884351>, 2025.

Dottori, F., Salamon, P., Bianchi, A., Alfieri, L., Hirpa, F. A., and Feyen, L.: Development and evaluation of a framework for global flood hazard mapping, *Advances in Water Resources*, 94, 87–102, <https://doi.org/10.1016/j.advwatres.2016.05.002>, 2016.

EDF R&D: Telemac-Mascaret, <http://www.opentelemac.org>, hydrodynamics and water quality modelling system, 2014.

Farr, T. G., Rosen, P. A., Caro, E., Crippen, R., Duren, R., Hensley, S., Kobrick, M., Paller, M., Rodriguez, E., Roth, L., Seal, D., Shaffer, S., Shimada, J., Umland, J., Werner, M., Oskin, M., Burbank, D., and Alsdorf, D.: The Shuttle Radar Topography Mission, *Reviews of Geophysics*, 45, <https://doi.org/10.1029/2005RG000183>, 2007.

García-Alén, G., Hostache, R., Cea, L., and Puertas, J.: Joint assimilation of satellite soil moisture and streamflow data for the hydrological application of a two-dimensional shallow water model, *Journal of Hydrology*, 621, 129 667, <https://doi.org/10.1016/j.jhydrol.2023.129667>, 2023.

Geuzaine, C. and Remacle, J.-F.: Gmsh: A 3-D finite element mesh generator with built-in pre- and post-processing facilities, *International Journal for Numerical Methods in Engineering*, 79, 1309–1331, <https://doi.org/10.1002/nme.2579>, 2009.

Godet, J., Nicolle, P., Hocini, N., Gaume, E., Davy, P., Pons, F., Javelle, P., Garambois, P.-A., Lague, D., and Payrastre, O.: Benchmark dataset for hydraulic simulations of flash floods in the French Mediterranean region, *Earth System Science Data*, 17, 2963–2983, <https://doi.org/10.5194/essd-17-2963-2025>, 2025.

GRASS Development Team: Geographic Resources Analysis Support System (GRASS GIS) Software, Version 8.2, Open Source Geospatial Foundation, [https://doi.org/https://doi.org/10.5281/zenodo.5176030](https://doi.org/10.5281/zenodo.5176030), 2022.

Hervouet, J.-M.: Hydrodynamics of free surface flows: Modelling with the finite element method, Wiley, <https://doi.org/DOI:10.1002/9780470319628>, 2007.

Hocini, N.: Evaluation de méthodes automatisées de cartographie des zones inondables adaptées à la prévision des crues soudaines, Ph.D. thesis, <http://www.theses.fr/2022NANU4015>, thèse de doctorat dirigée par Gaume, Eric et Payrastre, Olivier Renaud Sciences de la Terre et de l'environnement Nantes Université 2022, 2022.

Hocini, N. and Pons, F.: TELEMAC-2D Upgrades: Rainfall Spatialization and Control Sections, in: *Advances in Hydroinformatics, SimHydro 2023 Volume 2*, edited by Gourbesville, P. and Caaignaert, G., pp. 65–77, Springer Nature Singapore, Singapore, 2024.

Hocini, N., Payrastre, O., Bourgin, F., Gaume, E., Davy, P., Lague, D., Poinsignon, L., and Pons, F.: Performance of automated flood inundation mapping methods in a context of flash floods: a comparison of three methods based either on the Height Above Nearest Drainage (HAND) concept, or on 1D/2D shallow water equations, *Hydrology and Earth System Sciences Discussions*, 2020, 1–23, <https://doi.org/10.5194/hess-2020-597>, 2020.



775 Jenson, S. K. and Domingue, J. O.: Extracting topographic structure from digital elevation data for geographic information-system analysis, Photogrammetric Engineering and Remote Sensing, 54, 1593–1600, <https://pubs.usgs.gov/publication/70142175>, uSGS Publications Warehouse, 1988.

Kirstetter, G., Delestre, O., Lagrée, P.-Y., Popinet, S., and Josserand, C.: B-flood 1.0: an open-source Saint-Venant model for flash-flood simulation using adaptive refinement, Geoscientific Model Development, 14, 7117–7132, <https://doi.org/10.5194/gmd-14-7117-2021>, 2021.

Li, Z., Chen, M., Gao, S., Luo, X., Gourley, J. J., Kirstetter, P., Yang, T., Kolar, R., McGovern, A., Wen, Y., Rao, B., Yami, T., and Hong, 780 Y.: CREST-iMAP v1.0: A fully coupled hydrologic-hydraulic modeling framework dedicated to flood inundation mapping and prediction, Environmental Modelling Software, 141, 105 051, <https://doi.org/https://doi.org/10.1016/j.envsoft.2021.105051>, 2021.

Ligier, P.-L.: Implementation of a rainfall-runoff model in TELEMAC-2D, in: Proceedings of the XXIIIrd TELEMAC-MASCARET User Conference 2016, 11 to 13 October, edited by Bourban, S. H., pp. 13–19, Oxfordshire: HR Wallingford, 2016.

785 Monnier, J., Couderc, F., Dartus, D., Larnier, K., Madec, R., and Vila, J.-P.: Inverse algorithms for 2D shallow water equations in presence of wet dry fronts: Application to flood plain dynamics, Advances in Water Resources, 97, 11–24, <https://doi.org/10.1016/j.advwatres.2016.07.005>, 2016.

Neal, J., Schumann, G., and Bates, P.: A subgrid channel model for simulating river hydraulics and floodplain inundation over large and data sparse areas, Water Resources Research, 48, 2012.

790 Nguyen, P., Thorstensen, A., Sorooshian, S., Hsu, K., AghaKouchak, A., Sanders, B., Koren, V., Cui, Z., and Smith, M.: A high resolution coupled hydrologic–hydraulic model (HiResFlood-UCI) for flash flood modeling, Journal of Hydrology, 541, 401–420, <https://doi.org/https://doi.org/10.1016/j.jhydrol.2015.10.047>, flash floods, hydro-geomorphic response and risk management, 2016.

Pons, A. F., Bonnifait, L., Criado, D., Payrastre, O., Billaud, F., Brigode, P., Fouchier, C., Gourbesville, P., Kuss, D., Nouveau, N. L., Martin, 795 O., Martins, C., Nomis, S., Paquet, E., and Cardelli, B.: Consensus hydrologique de la tempête ALEX du 2 et 3 octobre 2020 dans les Alpes-Maritimes, LHB, 110, 2363 619, <https://doi.org/10.1080/27678490.2024.2363619>, 2024.

Pons, F. and Hocini, N.: Apport des nouvelles méthodes automatiques de calculs hydrauliques, exemple du principe, données d’entrée et cas d’usage de Cartino2D, in: Colloque SHF, Météopole Toulouse, Toulouse, France, poster 011, 2023.

Pons, F. and Hocini, N.: Dataset for Cartino2D paper, <https://doi.org/10.5281/zenodo.17778609>, 2025.

Pons, F., Delgado, J.-L., Guero, P., and Berthier, E.: EXZECO : A GIS and DEM based method for pre-determination of flood risk related to direct runoff and flash floods, in: 9th International Conference on Hydroinformatics, pp. 2063–2070, Tianjin, China, 2010.

800 Pons, F., Laroche, C., Fourmigue, P., and and, M. A.: Cartographie des surfaces inondables extrêmes pour la directive inondation : cas de la Nartuby, La Houille Blanche, 100, 34–41, <https://doi.org/10.1051/lhb/2014014>, 2014.

Pons, F., Alquier, M., Paya, E., Moulin, C., Panier, N., and Chollet, A.-E.: Premiers tests de la méthode Cartino2D sur le territoire de Toulon Provence Méditerranée, LHB, 107, 1–13, <https://doi.org/10.1080/00186368.2021.1912968>, 2021.

Pons, F., Alquier, M., and Paya, E.: Automatic 2D mapping of flash floods: which possibilities and limits? An illustration based on the 805 Cartino2D method, in: EGU General Assembly 2022, Vienna, Austria, <https://doi.org/10.5194/egusphere-egu22-7212>, 2022.

Posit team: RStudio: Integrated Development Environment for R, Posit Software, PBC, Boston, MA, <http://www.posit.co/>, 2025.

Prodanovic, P.: PPUTILS: A practical toolkit for terrain, free surface flow and wave modeling, 2017.

Pujol, L., Garambois, P.-A., and Monnier, J.: Multi-dimensional hydrological–hydraulic model with variational data assimilation for river networks and floodplains, Geoscientific Model Development, 15, 6085–6113, <https://doi.org/10.5194/gmd-15-6085-2022>, 2022.



810 Pujol, L., Garambois, P.-A., Delenne, C., and Perrin, J.-L.: Adjoint-based sensitivity analysis and assimilation of multi-source data for the inference of spatio-temporal parameters in a 2D urban flood hydraulic model, *Journal of Hydrology*, 643, 131 885, [https://doi.org/https://doi.org/10.1016/j.jhydrol.2024.131885](https://doi.org/10.1016/j.jhydrol.2024.131885), 2024.

Pujol, L., Chen, S., and Garambois, P.-A.: Gradient-based estimation of spatially distributed parameters of a shallow water 2D rainfall-runoff model, *Advances in Water Resources*, 202, 104 978, <https://doi.org/https://doi.org/10.1016/j.advwatres.2025.104978>, 2025.

815 QGIS Development Team: QGIS Geographic Information System, QGIS Association, <https://www.qgis.org>, 2025.

R Core Team: R: A Language and Environment for Statistical Computing, R Foundation for Statistical Computing, Vienna, Austria, <https://www.R-project.org/>, 2021.

Roux, H., Labat, D., Garambois, P. A., Maubourgues, M.-M., Chorda, J., and Dartus, D.: A physically-based parsimonious hydrological model for flash floods in Mediterranean catchment, *Nat. Hazards Earth Syst. Sci. J1-NHESS*, 161, 2567–2582, special Issue, 2011.

820 Sampson, C. C., Smith, A. M., Bates, P. D., Neal, J. C., Alfieri, L., and Freer, J. E.: A high-resolution global flood hazard model, *Water Resources Research*, 51, 7358–7381, <https://doi.org/https://doi.org/10.1002/2015WR016954>, 2015.

Sheffer, N. A., Rico, M., Enzel, Y., Benito, G., and Grodek, T.: The Palaeoflood record of the Gardon River, France: A comparison with the extreme 2002 flood event, *Geomorphology*, 98, 71–83, <https://doi.org/https://doi.org/10.1016/j.geomorph.2007.02.034>, the Geomorphological and Palaeohydrological Response of Fluvial Systems to Climatic, Human and Tectonic Controls, 2008.

825 Tarboton, D. G.: The analysis of river basins and channel networks using digital terrain data, Sc.d. thesis, Massachusetts Institute of Technology, Cambridge, MA, also available as Technical Report No. 326, Ralph M. Parsons Laboratory for Water Resources and Hydrodynamics, Department of Civil Engineering, M.I.T., 1989.

Trigg, M. A., Birch, C. E., Neal, J. C., Bates, P. D., Smith, A., Sampson, C. C., Yamazaki, D., Hirabayashi, Y., Pappenberger, F., Dutra, E., Ward, P. J., Winsemius, H. C., Salamon, P., Dottori, F., Rudari, R., Kappes, M. S., Simpson, A. L., Hadzilacos, G., and Fewtrell, T. J.: 830 The credibility challenge for global fluvial flood risk analysis, *Environmental Research Letters*, 11, 094 014, <https://doi.org/10.1088/1748-9326/11/9/094014>, 2016.

UNISDR: Global Assessment Report on Disaster Risk Reduction: Making Development Sustainable – The Future of Disaster Risk Management, [https://www.preventionweb.net/english/hyogo/gar/2015/en/gar-pdf/GAR2015\\_EN.pdf](https://www.preventionweb.net/english/hyogo/gar/2015/en/gar-pdf/GAR2015_EN.pdf), United Nations Office for Disaster Risk Reduction (UNISDR), 2015.

835 USDA, T.: United States Department of Agriculture Natural Resources Conservation Service Conservation Engineering Division, Technical Release 55: Urban Hydrology for Small Watersheds, <https://www.hydrocad.net/tr-55.htm>, 1986.

Ward, P. J., Jongman, B., Weiland, F. S., Bouwman, A., van Beek, R., Bierkens, M. F. P., Ligtvoet, W., and Winsemius, H. C.: Assessing flood risk at the global scale: model setup, results, and sensitivity, *Environmental Research Letters*, 8, 044 019, <https://doi.org/10.1088/1748-9326/8/4/044019>, 2013.

840 Ward, P. J., Jongman, B., Salamon, P., Simpson, A., Bates, P., De Groot, T., Muis, S., de Perez, E. C., Rudari, R., Trigg, M. A., and Winsemius, H. C.: Usefulness and limitations of global flood risk models, *Nature Climate Change*, 5, 712–715, <https://doi.org/10.1038/nclimate2742>, 2015.

Wing, O. E. J., Pinter, N., Bates, P. D., Kousky, C., Wobus, C., Roberts, J., and Jones, R.: National-scale flood risk assessment for the conterminous United States, *Nature Climate Change*, 8, 693–697, <https://doi.org/10.1038/s41558-018-0207-x>, 2018.

845 Wing, O. E. J., Bates, P. D., Quinn, N. D., Savage, J. T. S., Uhe, P. F., Cooper, A., Collings, T. P., Addor, N., Lord, N. S., Hatchard, S., Hoch, J. M., Bates, J., Probyn, I., Himsworth, S., Rodríguez González, J., Brine, M. P., Wilkinson, H., Sampson, C. C., Smith, A. M., Neal, J. C.,



and Haigh, I. D.: A 30 m Global Flood Inundation Model for Any Climate Scenario, *Water Resources Research*, 60, e2023WR036460, <https://doi.org/https://doi.org/10.1029/2023WR036460>, e2023WR036460 2023WR036460, 2024.

Winsemius, H. C., Van Beek, L. P. H., Jongman, B., Ward, P. J., and Bouwman, A.: A framework for global river flood risk assessments, 850 *Hydrology and Earth System Sciences*, 17, 1871–1892, <https://doi.org/10.5194/hess-17-1871-2013>, 2013.

Yamazaki, D., Kanae, S., Kim, H., and Oki, T.: A physically based description of floodplain inundation dynamics in a global river routing model, *Water Resources Research*, 47, <https://doi.org/https://doi.org/10.1029/2010WR009726>, 2011a.

Yamazaki, D., Kanae, S., Kim, H., and Oki, T.: A physically based description of floodplain inundation dynamics in a global river routing model, *Water Resources Research*, 47, 2011b.